



GEOHERMOMETRY AND CHEMICAL EQUILIBRIA OF GEOHERMAL FLUIDS FROM HVERAGERDI, SW-ICELAND, AND SELECTED HOT SPRINGS JIANGXI PROVINCE, SE-CHINA

Sun Zhanxue

East China Geological Institute,
Linchuan, Jiangxi 344000,
CHINA

ABSTRACT

Solute-mineral equilibrium studies suggest that geothermal fluids from wells are close to equilibrium with hydrothermal alteration minerals but boiling/degassing and mixing in upflow zones lead to departure from equilibrium for thermal waters from hot springs in the Hveragerdi high-temperature geothermal field, SE-Iceland. The solute geothermometers and the $\log(Q/K)$ method give subsurface temperatures ranging on average from 183 to 204°C which compare well with the measured aquifer temperatures. Gas geothermometers indicate subsurface temperatures at 180-260°C reflecting a temperature decreasing trend from north to south in this field. The temperature of the reservoir water was estimated to be about 210-260°C by applying three mixing models. By integration of water and steam geochemical studies with temperature logging data from wells, a conceptual model was constructed for the geothermal field.

The water chemistry and subsurface temperatures of two selected hot spring areas in Jiangxi Province, SE-China were also discussed. The chalcedony geothermometer gives subsurface temperatures of 70-100°C for the low-temperature geothermal areas. The cold water fraction is estimated from tritium concentration to be 20-30% in the mixed waters. Results of this study suggest that secondary carbonate minerals may be close to equilibrium with solution, although an overall equilibrium for mineral-solution is not attained in the low-temperature systems.

1. INTRODUCTION

The primary objective of an exploration and evaluation programme in a geothermal area is to determine as inexpensively and rapidly as possible the capacity to economically produce geothermal fluids for industrial exploitation. Geochemical techniques, applied during the various stages of exploration and evaluation as well as exploitation, are particularly important due to the information they supply at cost that is relatively low compared to that of geophysical methods and drilling. For the past several decades, water chemistry and gas composition of geothermal fluids have proved very effective in evaluating subsurface temperature, determining water origin, identifying and eliminating mixing effects, and

predicting scaling and corrosion (e.g. Fournier, 1977; Arnórsson et al., 1983a and b; Giggenbach, 1988; Ármannsson et al., 1986 and 1989; Ármannsson, 1989; Tole et al., 1993; Wang et al., 1993; Zhao Ping and Ármannsson, 1996; Marini et al., 1998).

In this report chemical analyses for geothermal fluids from the Hveragerdi high-temperature geothermal field, SW-Iceland, and some selected hot springs from Jiangxi Province, SE-China were used to evaluate the probable existing chemical equilibria and to estimate subsurface temperatures in geothermal systems. The mixing and boiling/degassing processes in up-flow zones below hot springs and boreholes were assessed using three mixing models. The subsurface temperatures predicted by various geothermometers are evaluated by comparison with measured downhole temperatures. Most calculations were performed with the SOLVEQ (Reed and Spycher, 1984; Spycher and Reed, 1989) and WATCH (Arnórsson et al., 1982; Bjarnason, 1994) programs.

2. SAMPLING AND ANALYSIS OF GEOTHERMAL FLUIDS

Sample collection, chemical analysis and data interpretation are the three main steps involved in geochemical studies of geothermal fluids. In this section, a brief description of the sampling techniques, sample treatment and analytical techniques adopted for this study will be given. Detailed information about sampling and analytical techniques in geothermal studies can be found e.g. in Ólafsson (1988), Paces (1991), and Arnórsson (1991).

2.1 Sampling techniques and sample treatment

The types of samples used in the study are water samples from springs and hot water wells, steam samples from fumaroles, and steam and water samples from wet-steam wells.

To sample hot springs and hot water wells, it is generally satisfactory to use a can of about 1 litre volume made of PVC, or similar material, to scoop samples from large springs. However, whenever a gravity flow can be sustained, water samples should be collected with the aid of a funnel and silicone tubing. Samples for determination of pH and CO₂ should be cooled to about ambient temperature and subsequently collected into a gas sampling bulb. This is done by connecting a cooling coil of stainless steel to the silicone tubing and inserting it into a bucket with cold water.

To sample fumaroles, it is necessary to measure the temperature at different locations and select an appropriate steam vent. When a sampling outlet has been selected, the funnel is placed upside-down over the outlet and covered well with moist hydrothermal clay to avoid atmospheric contamination. If possible, it is convenient to have a gravity driving flow of water from the sampling spot and through the cooling device. Otherwise, a vacuum pump is needed.

The collection of representative gas samples from a discharging well involves the collection of dry gas (non-condensable gases), condensate, steam (in NaOH solution) and hot water. It should be conducted with the aid of a Webre separator and a cooling device. Great care should be taken to separate steam completely from liquid.

Sample treatment is specific for particular analytical methods (Table 1). Usually, the water samples were collected in several fractions. Ru samples are raw and untreated for CO₂ and H₂S analysis, Rd ones are raw and diluted on site with de-ionized water to bring SiO₂ below 100 ppm for SiO₂ analysis, Fu ones are filtered and untreated for anion analysis, Fp ones are filtered and precipitated for SO₄ analysis and Fa ones are filtered and acidified with 1 ml "suprapur" HNO₃ added to 500 ml sample for metal element analysis.

2.2 Analytical chemical methods

The analytical methods used to obtain the data for the report are presented in Table 1. All chemical data are reported in the relevant sections.

TABLE 1: Analytical methods for geothermal fluids

Constituents	Sample fraction	Analytical method
H ₂ S	Ru	Titration with 0.001 MHgAc ₂ solution and dithizone indicator
pH, CO ₂	Ru	Titration, HCl/pH-titrator
SiO ₂	Rd	Spectrophotometer (ammonium molybdate used)
Na, K	Fa	Atomic absorption spectrophotometer (flame, Cs added)
Ca, Mg	Fa	Atomic absorption spectrophotometer (flame, La added)
Al	Fa	Atomic absorption spectrophotometry-graphite furnace
Fe	Fa	Atomic absorption spectrophotometer-flame
SO ₄	Fp	Ion chromatography
Cl	Fu	Ion chromatography
B	Fu	Spectrophotometer (azomethine-H used)
F	Fu	Selective electrode

3. CHEMICAL EQUILIBRIA AND GEOTHERMOMETRY

The prediction of subsurface temperatures using chemical geothermometers is one of the major applications of geochemistry to the exploration for geothermal resources. Chemical geothermometers are based on the assumption that a temperature-dependent equilibrium is attained in the geothermal reservoir between specific solution(s)-gas(es) and mineral(s), or specific gas-gas equilibria in the case of some gas geothermometers.

3.1 Solute geothermometers

Since the 1960's, various solute geothermometers have been developed to predict subsurface temperatures in geothermal systems, such as silica geothermometers (e.g. Fournier and Rowe, 1966; Fournier, 1977; 1979a; Arnórsson and Svavarsson, 1985), Na-K geothermometers (e.g. Truesdell, 1976; Fournier 1979a; Arnórsson et al., 1983b; Giggenbach, 1988), Na-K-Ca geothermometer (Fournier and Truesdell, 1973) and Na-K-Ca-Mg geothermometer (Fournier and Potter, 1979; Giggenbach, 1988).

As mentioned above, these geothermometers are all based on the attainment of chemical equilibria in geothermal systems. When applied to the same geothermal fluid, the different geothermometers frequently yield appreciably different subsurface temperatures due to lack of equilibrium between the solution and hydrothermal minerals, or as a result of reactions, mixing or degassing during up-flow. In order to get reasonable results, the validity of the assumptions of specific solution/mineral equilibria, and some of the physical and chemical processes involved should be taken into account. The solute geothermometers used in this report are listed here below.

Chalcedony geothermometer, 0-250°C (Fournier, 1977):

$$t(^{\circ}\text{C}) = \frac{1032}{4.69 - \log \text{SiO}_2} - 273.15 \quad (1)$$

Quartz geothermometer, 0-250°C (Fournier and Potter, 1982):

$$t(^{\circ}\text{C}) = -42.198 + 0.28831 \text{SiO}_2 - 3.6686 \times 10^{-4} (\text{SiO}_2)^2 + 3.1665 \times 10^{-7} (\text{SiO}_2)^3 + 77.034 \log \text{SiO}_2 \quad (2)$$

Na/K geothermometer, 25-250°C (Arnórsson, et al., 1983b):

$$t(^{\circ}\text{C}) = \frac{933}{0.993 + \log(\text{Na/K})} - 273.15 \quad (3)$$

Na-K-Ca geothermometer, 4-340°C (Fournier and Truesdell, 1973):

$$t(^{\circ}\text{C}) = \frac{1647}{\log(\text{Na/K}) + \beta [\log(\sqrt{\text{Ca/Na}}) + 2.06] + 2.47} - 273.15 \quad (4)$$

$\beta = 4/3$ for $t < 100^{\circ}\text{C}$; $\beta = 1/3$ for $t > 100^{\circ}\text{C}$

3.2 Fluid-mineral equilibria and calculations

Calculation of multi-component fluid-mineral equilibria in geothermal systems and its application to geothermometry was proposed by Reed and Spycher (1984). For the dissolution of a mineral m , the saturation index $\log(Q_m/K_m)$ can be written as

$$\log(Q_m/K_m) = \log\left[\left(\prod a_{i,m}^{\nu_{i,m}}/a_m\right)/K_m\right] \quad (5)$$

where $a_{i,m}$ is the activity and $\nu_{i,m}$ is the stoichiometric coefficient of species i for mineral m . The reaction equation is written with the mineral on the left hand side, and the aqueous components on the right hand side, the activity of mineral m , a_m , being equal to one for pure minerals; K_m is the equilibrium constant for mineral m at a specific temperature.

In a plot of $\log(Q_m/K_m)$ vs. temperature, all plausible alteration minerals in equilibrium with the solution in the geothermal system will converge to a value of 0 at the same temperature. The temperature can be regarded as equilibrium or reservoir temperature.

As Arnórsson (1991) pointed out, the thermodynamic data for many commonly occurring hydrothermal minerals are subject to considerable uncertainty, and many of them form solid solutions. Both these factors produce an uncertainty in the calculated $\log(Q_m/K_m)$ values for these minerals and therefore, in the calculated equilibrium temperatures. Interpretation of data in $\log(Q_m/K_m)$ vs. temperature diagrams must also take into account the fact that the mineral assemblage with which the water appears to have equilibrated must be an assemblage that is logical in terms of field observations, i.e. it must not contain minerals which are known to be unstable at the predicted temperature.

3.3 Gas geothermometers and equilibria associated with gases

In many geothermal fields, surface manifestations consist of fumaroles, steam-heated waters, and hot altered ground. The solute geothermometers are not applicable to the exploration of such fields. Since the 1970's, studies have successfully demonstrated that gas components from fumaroles or well discharges can be used as geothermometers (e.g. Tonani, 1973; Arnórsson and Gunnlaugsson, 1985; D'Amore, 1991; Giggenbach, 1991). In this report, the five gas geothermometers from Arnórsson (1991)

were applied to fumarole steam and steam from wet-steam wells in the Hveragerdi high-temperature geothermal field as follows (conc. in mmoles / kg steam):

CO₂ geothermometer, at temperature range 100-330°C:

$$T_{CO_2} = -44.1 + 269.25 \log m_{CO_2} - 76.88 (\log m_{CO_2})^2 + 9.52 (\log m_{CO_2})^3 \quad (6)$$

H₂S geothermometer, at temperature range >100°C:

$$T_{H_2S} = 173.2 + 65.04 \log m_{H_2S} \quad (7)$$

H₂ geothermometer, at temperature range >100°C:

$$T_{H_2} = 212.1 + 38.59 \log m_{H_2S} \quad (8)$$

CO₂/H₂ geothermometer, at temperature range >100°C:

$$T_{CO_2/H_2} = 311.7 - 66.72 \log(m_{CO_2}/m_{H_2}) \quad (9)$$

CO₂/N₂ geothermometer, at temperature range >100°C:

$$T(^{\circ}C) = 148.5 + 64.35 \log(m_{CO_2}/m_{N_2}) + 5.239 [\log(m_{CO_2}/m_{N_2})]^2 - 1.832 [\log(m_{CO_2}/m_{N_2})]^3 \quad (10)$$

Geothermal gases are originally introduced into the geothermal fluid with recharge water from water-rock interaction in the reservoir or from a magmatic fluid invasion. In an undisturbed reservoir, reactions in equilibrium at the reservoir temperature control the concentrations of these gases.

The temperature equations for the gas geothermometers presented above are considered to correspond with equilibria between the respective gases and specific mineral buffers. Calcite, together with quartz, epidote and prehnite above about 230°C, and various zeolites in addition to calcite may possibly be involved at lower temperatures (Arnórsson and Gunnlaugsson, 1985). Iron minerals and iron-containing aluminium silicates such as pyrite + pyrrhotite + epidote + prehnite, magnetite + epidote + prehnite and/or pyrite + epidote + prehnite + chlorite may constitute the H₂S and H₂ buffers (Giggenbach, 1980; Arnórsson and Gunnlaugsson, 1985).

4. THE HVERAGERDI HIGH-TEMPERATURE GEOTHERMAL FIELD, SW-ICELAND

4.1 General background

Iceland is located on the Mid-Atlantic Ridge which traverses the island from southwest to northeast where the active spreading axis appears as a zone of active rifting and volcanism. The volcanic rift zone is characterized by active volcanoes, fissure swarms, numerous normal faults and high-temperature geothermal fields. Geothermal activity in Iceland is divided into two types on the basis of the base temperature (maximum temperature) in the uppermost 1 km. The base temperature is thus $\leq 150^{\circ}C$ in the low-temperature areas, but $\geq 200^{\circ}C$ in the high-temperature areas. Low-temperature fields are in Plio-Pleistocene and Tertiary volcanics, and the high-temperature fields are located in the active volcanic zones (Fridleifsson, 1979).

The Hveragerdi high-temperature geothermal field, located about 50 km southwest of Reykjavik, is on the southern margin of the Hengill neovolcanic area. Numerous drillholes have been sunk into the field (Figure 1). A temperature reversal is observed in most of the wells and a temperature decrease from a maximum of 230°C in the northern part of the drilled area to about 160°C just south of the Hveragerdi village. This temperature reversal has been explained by lateral flow from the central parts of the Hengill geothermal area. The δD value of thermal water in the field is around -65‰ (SMOW) which is considerably higher than those in neighbouring Nesjavellir and Ölkelduháls areas but similar to that at Kolvidarhóll (in Hengladalur) which is the westernmost geothermal field in the Hengill area. This suggests that the water in Hveragerdi and Kolvidarhóll does not originate as far inland as that in the other two areas (Ármannsson, pers. comm.).

In the Hveragerdi field, geothermal manifestations consist of fumaroles dominating in the north, and hot springs most abundant in the south. The sampling locations for samples used in this report are shown in Figure 1.

In the geothermal field, subsurface temperature estimations by water and gas chemistry from hot springs, well discharges and fumaroles have been made by Arnórsson and Gunnlaugsson (1985); Gestsdóttir and Geirsson (1990); Geirsson and Arnórsson (1995); and Ívarsson (1996). However, except for well 4 (Reed and Spycher, 1984), no detailed studies on mineral-solution equilibria in the field have been performed, and further interpretation of available data by integration of gas and water geochemistry also needs to be made. In this report, some of these tasks will be tackled.

4.2 Water chemistry

The analytical chemical results for samples from springs and wet-steam wells in the Hveragerdi geothermal field are presented in Tables 2 and 3. The chemical composition of the waters is investigated in terms of relative Cl, SO₄ and HCO₃ concentrations (Figure 2a), and relative Na+K, Ca and Mg concentrations (Figure 2b). Inspection of these plots points to the occurrence of the following two hydrochemical types of waters:

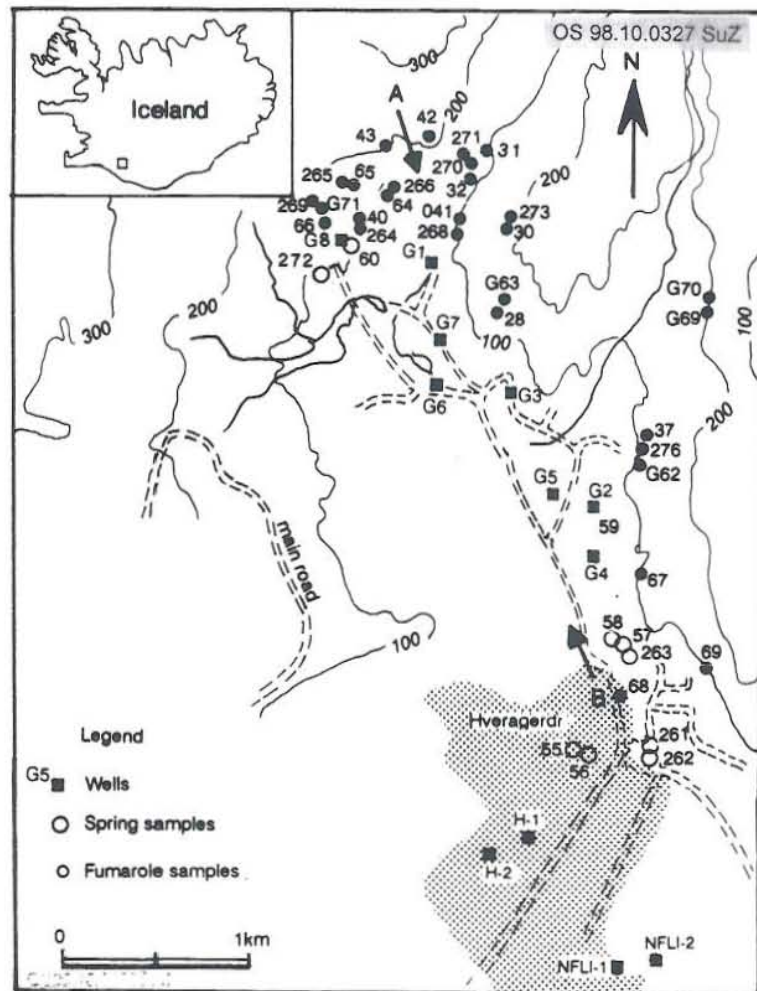


FIGURE 1: The Hveragerdi high-temperature field, SW-Iceland; location of wells, fumaroles and hot springs included in the report

TABLE 2: Chemical composition of spring discharges in the Hveragerdi geothermal field (concentrations in ppm)

No.	55	56	57	58	59	60	261	262	263	272	275	3018	9176	8214	8751
T (°C)	83.0	93.5	95.0	100	73.5	98.0	93.8	92.3	97.3	43.0	97.5	12	6.4	6.0	2.4
Q (l/s)	3.0	0.2	3.0	0.1	0.2	1.0	0.5	0.8	1.0	5.0	0.4	nd	nd	nd	nd
pH/°C	9.14/27	9.06/26	9.35/27	8.88/27	7.43/27	9.01/27	8.71/17	7.74/20	7.49/22	7.16/23	8.90/22	7.57/24	7.92/21	7.33/20	7.95/23
SiO ₂	355.3	161.5	272.5	328.2	381.3	262.6	223.0	182.6	159.9	66.7	310.2	31.7	16.5	25.46	14.41
B	0.678	0.622	0.765	0.573	0.431	0.853	0.534	0.403	0.233	0.016	0.629	0.02	0.016	nd	nd
Na	190.51	180.72	187.35	166.28	131.58	199.83	154.47	129.70	117.00	71.22	176.23	14.6	8.57	17.61	10.21
K	11.77	12.88	11.16	9.45	6.29	15.00	6.58	6.02	6.32	7.40	11.36	1.22	0.62	1.26	0.40
Ca	2.23	1.95	1.71	1.95	15.25	1.93	4.87	10.37	8.36	21.06	2.14	7.12	5.52	9.94	7.33
Mg	0.035	0.017	0.007	0.015	1.528	0.278	0.097	0.422	0.796	8.255	0.187	3.0	2.04	3.18	0.982
ΣCO ₂	62.7	54.5	42.4	78.8	122.4	73.0	47.5	76.6	128.9	141.0	83.80	41.6	19.2	43.3	25.8
SO ₄	74.9	59.7	50.5	53.7	33.5	31.4	55.9	45.00	48.7	11.3	69.7	10.0	3.99	7.59	2.49
ΣH ₂ S	0.54	2.85	5.27	3.69	0.15	2.35	5.64	3.16	1.70	0.04	4.58	0.01	0	0.05	0.03
Cl	158.1	152.9	165.6	130.9	115.5	197.7	147.3	112.6	59.2	8.4	138.4	16.8	11.7	13.06	9.31
F	2.099	2.012	2.097	1.533	1.269	1.147	1.630	1.144	0.876	0.114	1.865	0.05	0.05	0.089	0.074
Source	[1]	[1]	[1]	[1]	[1]	[1]	[1]	[1]	[1]	[1]	[1]	[1]	[2]	[2]	[2]

[1]: Data from Gestsdóttir and Geirsson (1990);
 [2]: Data from Orkustofnun data base; nd-not determined.

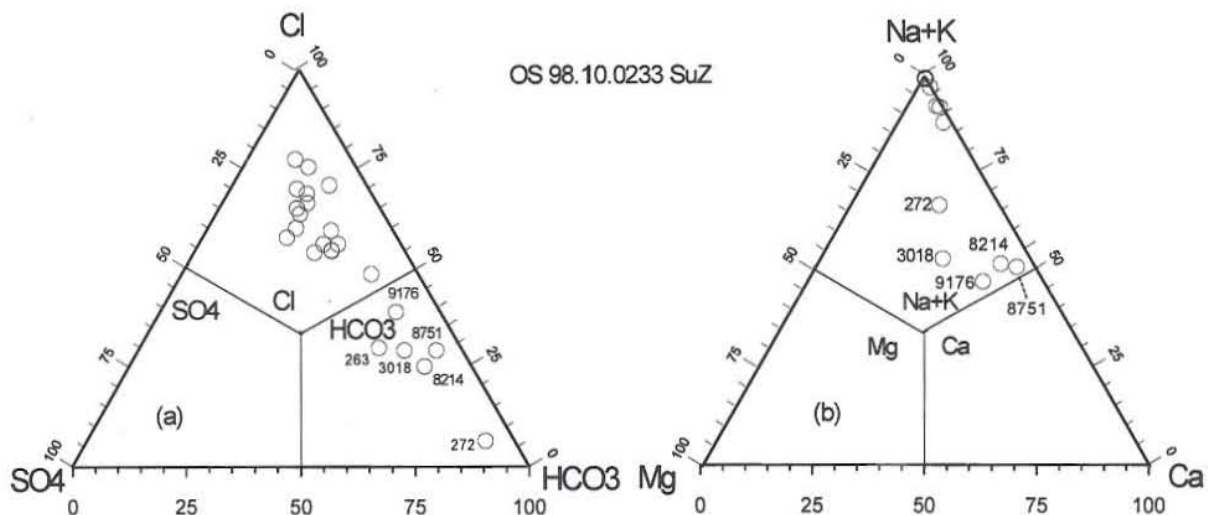


FIGURE 2: The triangular diagrams of relative component concentrations (in equivalents) for the Hveragerdi waters, a) Relative Cl, SO₄- and HCO₃ concentrations; and b) Relative Na + K, Ca and Mg concentrations

- The first type is **Na-HCO₃ water**. The group includes 6 samples, numbered 9176, 8751, 8214 and 3018 from cold springs, and 263 and 272 from hot springs. From all the hot springs sampled in the field, hot spring sample No. 272 has the lowest Cl, SO₄, B and silica but highest Mg concentrations. The water is probably steam-heated. Considering its temperature and low chloride and boron concentrations, hot spring no. 263 is probably steam-heated water, too.
- The second type is **Na-Cl water**. This type of water is found in all the thermal discharges except the two above-mentioned hot springs. The discharges from wells are probably representative of deep, undiluted geothermal fluids. To some extent, the deep Na-Cl waters are affected by

dilution with shallow low-salinity waters, as shown by the correlation plot between the conservative (mobile) species Cl and B (Figure 3a). In this diagram, all the waters plot along a linear trend joining the Cl-rich and B-rich waters and the Cl-poor and B-poor waters. A similar spread of points is observed in the B vs. SiO₂, F vs. Cl, Cl vs. K, Cl vs. Na and Cl vs. SiO₂ plots (Figure 3), but the results are more scattered probably due to re-equilibration of mixed Na-Cl waters with rocks at decreasing temperatures, and precipitation of solid phases upon degassing and/or boiling.

TABLE 3: Chemical composition of wet-steam well discharges in the Hveragerdi high-temperature field (concentrations in ppm)

Well no.	G2	G4	G6	G7	NLFI-1	NLFI-2	H-1	H-2
Sample no.	79-136	79-32	83-013	81-017	82-0090	82-0091	78-0082	79-0003
Water sample								
pH/°C	9.29/19	8.82/20	9.05/20	8.86/20	8.38/24.5	8.45/24.5	9.28/21	9.31/18
SiO ₂	259	281	425.6	425.9	235.9	260.75	280	340
B		0.62	0.95	0.99				
Na	168.0	153.3	164.2	176.8	160	160	189	167
K	13.8	13.4	20.72	21.28	11.05	12.25	9.2	12.7
Ca	2.18	1.73	2.15	1.68	1.62	1.86	2.08	2.05
Mg	0.002	0.002	0.021	0.008	0.002	0.003	0.007	0
∑CO ₂	44.2	74.2	28.6	43.4	87.8	77.0	49	45.6
SO ₄	40.0	43.7	37.2	35.2	43.5	42.34	70.3	41.5
∑H ₂ S	18.4	19.2	23.4	23.4	15.5	18.50	17	22.1
Cl	142.3	109.5	171.2	186.3	130.17	135.67	124	132
F	1.68	1.82	0.96	0.62	1.516	1.741	1.78	1.87
Fe		0.008	0.006	0.005				
Al		0.14			0.48	0.52		
Steam sample (mmoles/kg)								
CO ₂	32.26	51.49	56.41	69.82	56.96	83.51	65.16	65.99
H ₂ S	4.43	3.81	2.68	6.04	6.31	5.98	5.24	6.37
H ₂	0.699	1.23	1.39	1.27	1.29	1.26	1.43	1.85
CH ₄	0.072	0.132	0.094	0.150	0.15	0.17	0.17	0.15
N ₂	0.021	4.14	22.32	19.12	3.87	4.16	0	0
Ar			0.306	0.980	0.07	0.07		
Sampling Pressure	5.5	6.8	10.0	12.0	4.4	6.4	6.4	6.8
Aquifer T. (°C)	182	181	215	225	169	168	178	181
Source	[1]	[2]	[1]	[1]	[3]	[3]	[3]	[3]

[1]: Arnórsson (1985); [2]: Arnórsson et al., (1983a); [3]: Orkustofnun data base.

In order to identify the equilibrium status of the geothermal fluids, the Na-K-Mg triangular diagram (Giggenbach, 1988) was drawn (Figure 4). The data in Figure 4 fall mainly into three groups: 1) Immature waters, the cold springs no. 8214, 9176, 8751 and 3018, hot spring 59 and two steam-heated waters no. 263 and 272; 2) Equilibrated and nearly equilibrated waters, the well discharges, no. H-1, G2, NLFI-1, NLFI-2, G4, and hot spring 57; 3) Mixed and boiled/degassed waters, hot springs no. 261, 262, 275, 55, 56, 58 and 60, and well samples no. G6 and G7. Besides these, well discharge sample H-2, plotting above the full equilibrium line, is probably due to steam loss/degassing and the Mg concentration being smaller than the detection limit of the method used. Clearly, the use of cation geothermometers for most well discharges in the field is justified. The mixed and degassed/boiled waters will be discussed later.

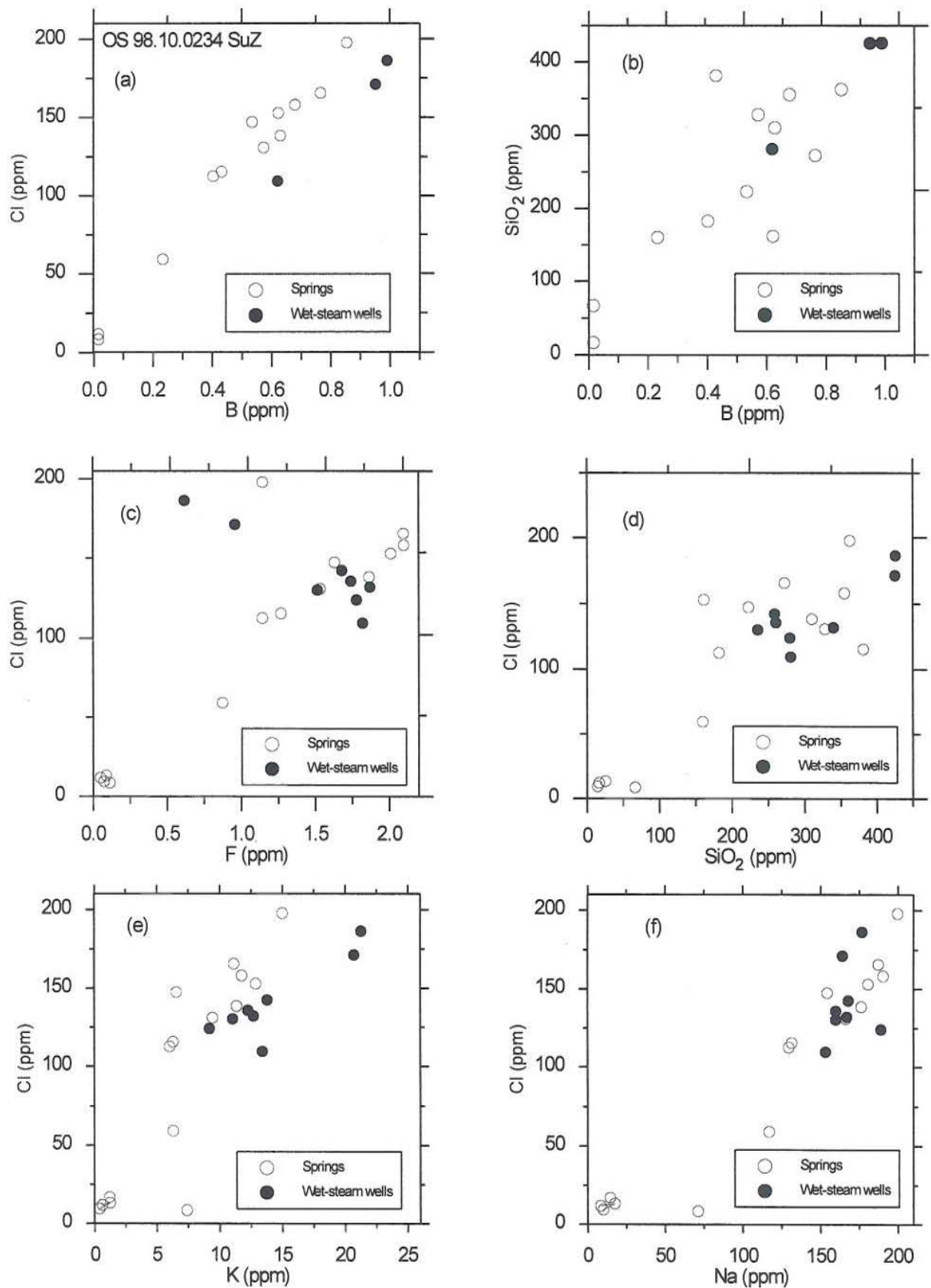


FIGURE 3: Correlation plots between various constituents, a) B vs. Cl; b) B vs. SiO₂; c) F vs. Cl; d) Cl vs. SiO₂; e) Cl vs. K; and f) Cl vs. Na

4.3 Subsurface temperature estimation

4.3.1 Solute geothermometry results

As mentioned in Section 3.1, the silica, Na-K and Na-K-Ca geothermometers are used to estimate subsurface temperatures in the geothermal field based on data from hot springs and well discharges by applying the respective equations given there. These solute geothermometry results for hot springs and well discharges are reported in Table 4 and Figure 5.

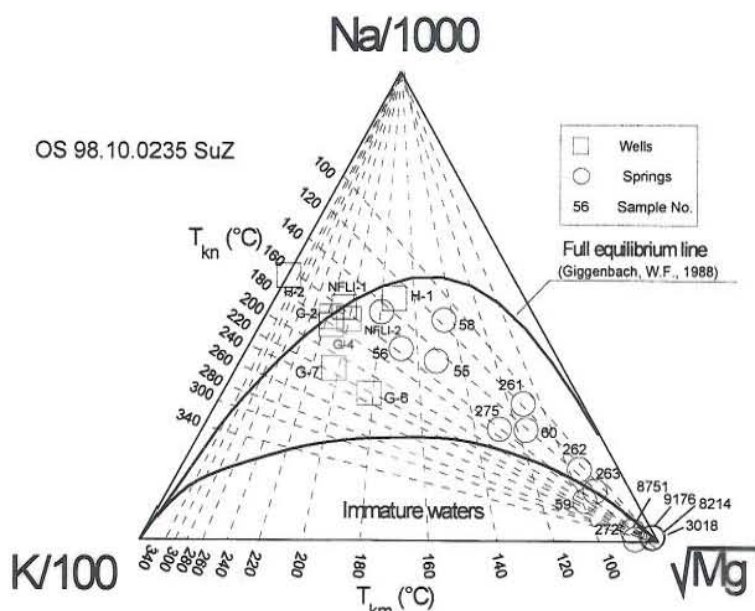


FIGURE 4: The Na-K-Mg triangular diagram for the Hveragerdi waters

TABLE 4: The results of solute geothermometry and mineral equilibrium calculations using the WATCH and SOLVEQ computer programs

Sample no.	T _{mea} (°C)	T _{quartz} (°C)	T _{chalced.} (°C)	T _{NaK} (°C)	T _{NaKCa} (°C)	Equil.temp. range (°C)	Cluster equil. temp. (°C)	Best equil. temp. (°C)
Wells								
G2	182	188	167	180	188	160-190	170-190	185
G4	181	200	181	188	192	130-210	160-180	170
G6	215	230	215	228	213	125-215	170-215	210
G7	225	234	219	223	215	190-225	225	225
NLFI-1	169	190	169	164	185	180-215	180-200	190
NLFI-2	168	197	177	175	180	170-210	180-205	190
H-1	178	189	169	133	163	170-210	178-210	178
H-2	181	205	187	175	184	180-200	185-200	185
Springs								
55	83	208	190	155	175	25-210	nc	nc
56	93.5	156	131	168	183	100-190	nc	nc
57	95	181	156	151	175	50-200	nc	nc
58	100	209	191	146	169	80-220	nc	nc
59	73.5	230	216	131	93	60-240	nc	nc
60	98	189	168	173	188	60-220	nc	nc
261	93.8	185	164	na	146	50-190	nc	nc
262	92.3	174	151	129	142	50-180	nc	nc
263	97.3	165	142	141	149	50-170	nc	nc
272	43	116	87	207	85	40-120	nc	nc
275	97.5	206	188	158	126	60-210	nc	nc

Quartz, chalcedony and Na-K geothermometer results are calculated by WATCH, Na-K-Ca temperature and mineral equilibrium temperature are calculated by SOLVEQ; na: not applicable; nc: no cluster found

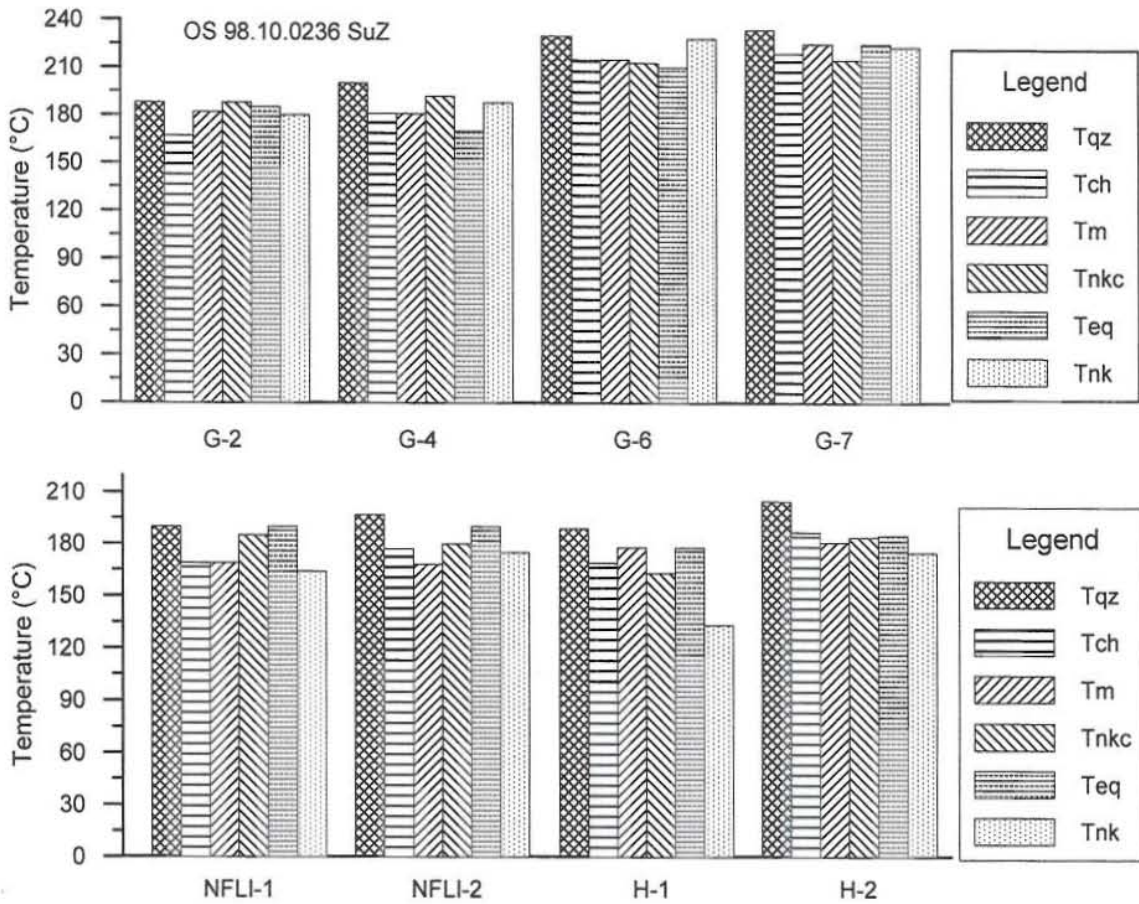


FIGURE 5: Comparison of various geothermometer temperatures with measured aquifer temperature

It can be seen from Table 4 and Figure 5 that the measured aquifer temperatures in wells and the four solute geothermometer temperatures compare quite well. On average, the quartz geothermometer yields 16.7°C higher values, the Na-K geothermometer gives 4.1°C lower values, and the Na-K-Ca geothermometer gives 2.6°C higher values. For all well discharges in the area, regardless of whether their aquifer temperatures are above or below 180°C, the chalcedony geothermometer gives excellent results which is only 1.9°C below the average measured temperatures. It may be inferred that chalcedony rather than quartz predominately controls the silica-fluid equilibrium in the geothermal system.

Solute geothermometer temperatures for all the hot springs except two steam-heated waters (Springs 272 and 263) are 165-230°C by the quartz geothermometer, 131-216°C by the chalcedony geothermometer, 129-173°C by the Na-K geothermometer, and 126-188°C by the Na-K-Ca geothermometer. The considerably large range of estimated subsurface temperatures is probably due to mixing and degassing/boiling effects as is already reflected in Figure 4. The detection and elimination of mixing and degassing/boiling effects will be discussed later.

4.3.2 Log(Q/K) diagrams

Firstly, the ionic balance for all data considered in the area was evaluated, and data with less than 10% difference between cation and anion concentration were selected for the study. Secondly, the saturation indices with respect to a number of hydrothermal minerals potentially present in the geothermal system were calculated at varying temperatures by means of SOLVEQ. The plausible alteration minerals in the

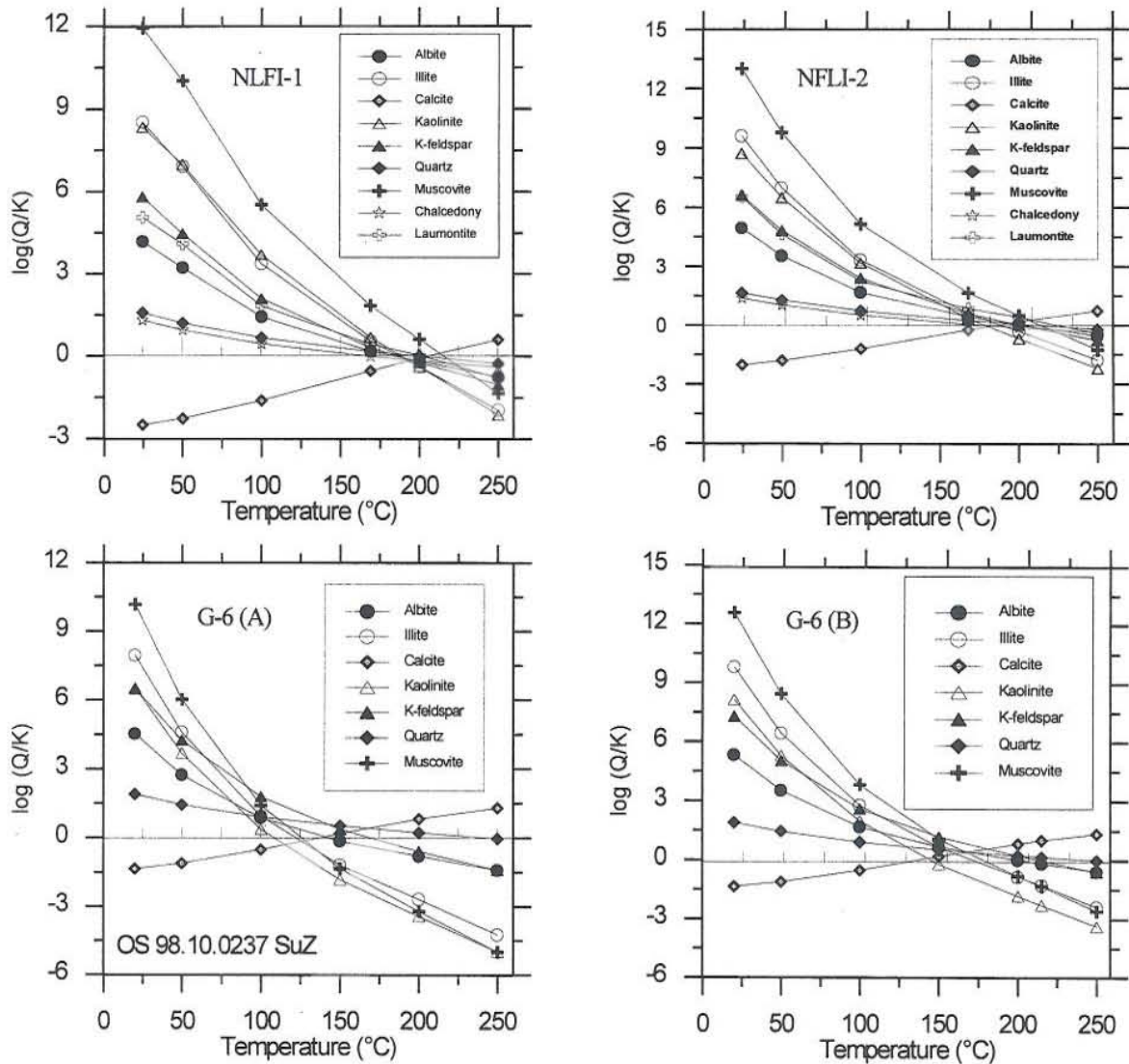


FIGURE 6: Log(Q/K) vs. temperature diagrams for wells, NLFI-1, NLFI-2 and G6, in the Hveragerdi field; G6 (a) is the original log(Q/K) graph, while G6(b) is the graph after estimation of Al concentration for G6

system were selected with reference to some available records of alteration minerals in the feed zones of the wells (Sigvaldason, 1962; Arnórsson et al., 1983a). Thirdly, the aluminium and iron values for some samples for which Al and Fe analyses were not available were estimated assuming that aluminium and iron concentrations were constrained by equilibrium with microcline and magnetite, respectively, using the forced-equilibrium method (Spycher and Reed, 1989; Pang and Reed, 1998). Finally, the log(Q/K) values were recalculated by adding the estimated Fe and Al values.

Log(Q/K) vs. temperature diagrams for some representative well discharges are shown in Figures 6-8. These diagrams show that solute-mineral equilibria for well discharges in the field seem to be attained or nearly attained. The range of equilibrium temperatures, the cluster equilibrium temperature and the best equilibrium temperature obtained by the log(Q/K) vs temperature diagrams for the data from the Hveragerdi high-temperature geothermal field are shown in Table 4, and Figure 5. It should be noted that the range of equilibrium temperatures, the cluster equilibrium temperature and the best equilibrium temperature, were arbitrarily defined as the temperature interval between minimum and maximum

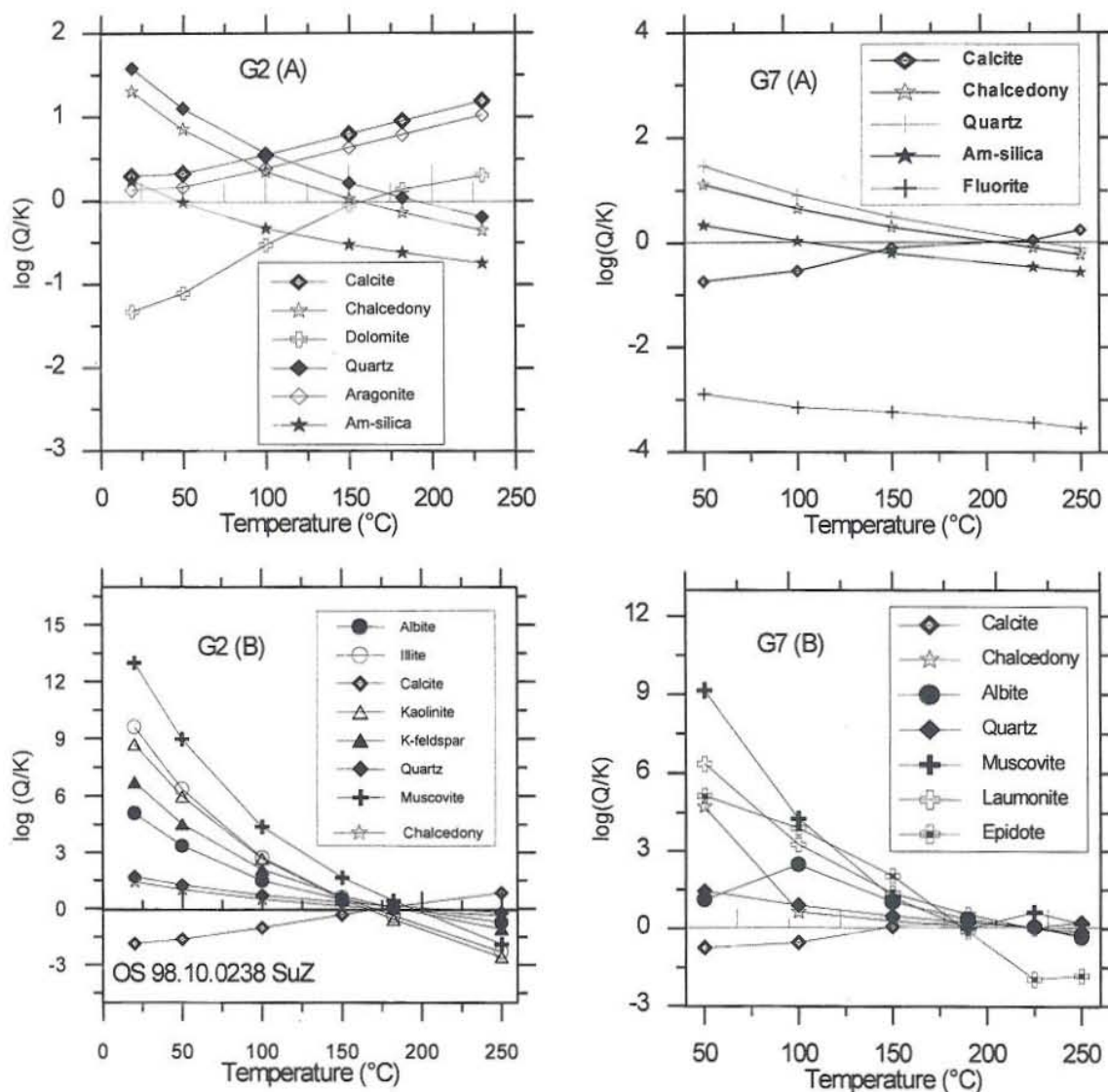


FIGURE 7: Log(Q/K) vs. temperature diagrams for the Hveragerdi well discharges; G2(a) is the original graph, while G2(b) is the graph after estimation of Al concentration for G2; G7(a) and G7(b) are the original graph, and the graph after estimation of Al and Fe concentrations, respectively.

equilibrium temperature for selected minerals, the temperature range over which most minerals appear to attain equilibrium, and the temperature at which the greatest number of minerals is in equilibrium with the aqueous solutions, respectively (Tole et al., 1993).

For well discharges, the best equilibrium temperatures compare quite well with the measured temperatures. On average, this method gives only 4.2°C higher values than the measured temperatures.

In order to compare the results calculated by two commonly used geothermal geochemical codes WATCH and SOLVEQ, the log(Q/K) vs temperature diagrams for G4 (Figure 8) were calculated both by WATCH and SOLVEQ. The range of equilibrium temperatures obtained by WATCH is about 140-220°C, and that obtained by SOLVEQ about 140-210°C. The best equilibrium temperatures obtained

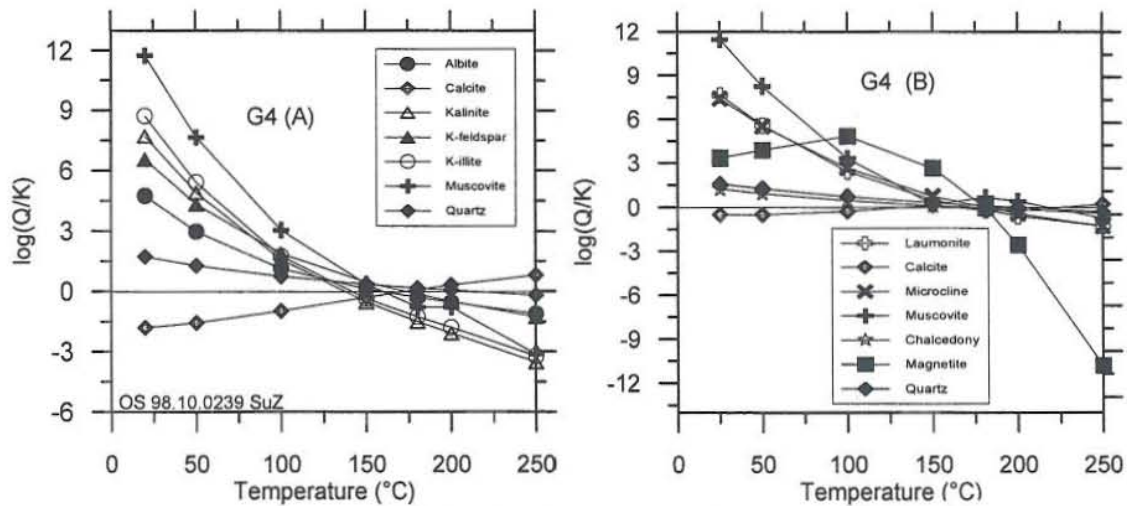


FIGURE 8: The $\log(Q/K)$ vs. temperature diagrams for well G4; G4(A) is obtained by SOLVEQ, and G4(B) obtained by WATCH

by the two programs for G4 are both around 170°C. So no significant difference was found between the results obtained by the two programs.

The $\log(Q/K)$ vs. temperature diagrams for some representative hot springs in the field are shown in Figure 9. In the diagram, no best equilibrium temperatures can be found probably owing to mixing, degassing/boiling and other relevant processes such as the precipitation of some minerals. It is interesting to note that the equilibrium temperatures for quartz and chalcedony in these $\log(Q/K)$ vs. temperature diagrams are almost the same as the estimated temperatures obtained by quartz and chalcedony geothermometers respectively in most cases. So $\log(Q/K)$ vs. temperature diagrams seem to be useful for predicting subsurface temperatures in this way.

4.4 Detection and elimination of mixing and degassing effects

As discussed in Section 4.2, most of the hot springs sampled are believed to contain waters of mixed origin. Such mixing can be detected from the following evidence: 1) The measured temperatures for these springs are 33-146°C below the calculated geothermometer temperatures in all cases; 2) Linear relationships between Cl and B as well as F, SiO₂, K, Na, also between B and SiO₂, exist as shown in Figure 3; 3) Most of the hot spring waters fall into the mixed waters section of the Na-K-Mg triangular diagram (Figure 4).

The evident mixing processes diminish the reliability of the subsurface temperatures estimated by solute geothermometers. In order to eliminate such mixing effects, three mixing models have been applied to evaluate the subsurface temperatures of the Hveragerdi geothermal system.

The silica-enthalpy warm spring model (Truesdell and Fournier, 1977) is based on the silica-enthalpy relationship of hot spring waters. It assumes that conductive cooling and changes in aqueous silica concentrations do not occur in the up-flow subsequent to mixing. Figure 10a shows the results of this model applied to the Hveragerdi data. The hot water component of the mixed hot spring waters is expected to be 220-237°C. In Figure 10a, line a is based on sample 55 which has the highest silica concentration and assumes adiabatic cooling to 100°C prior to mixing whereas line b assumes conductive cooling for hot spring 56 in which the silica concentration is the lowest except for the two steam-heated waters, no. 263 and 272.

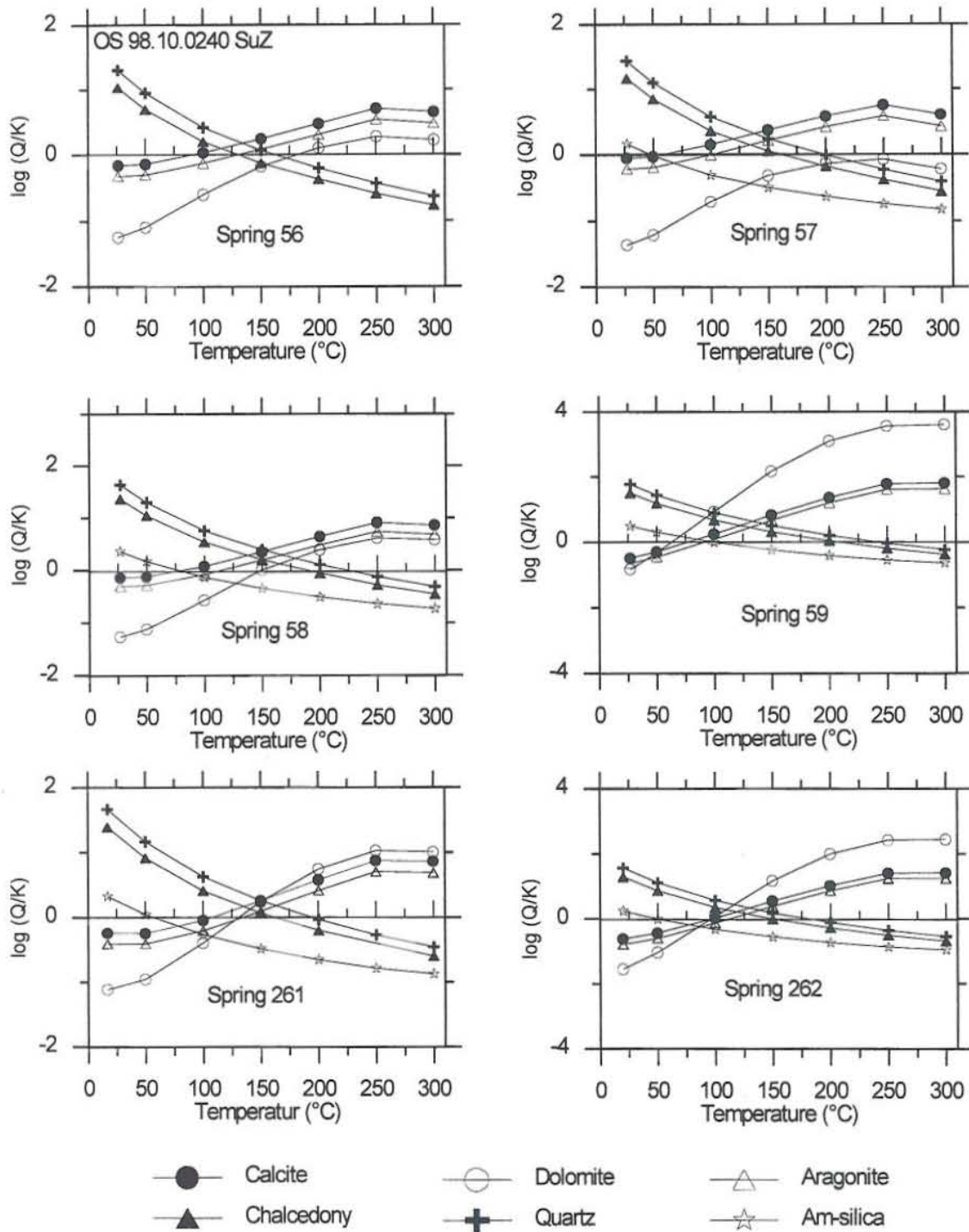


FIGURE 9: Log(Q/K) vs. temperature diagrams for hot springs 56, 57, 58, 59, 261 and 262

The carbonate-silica mixing model (Arnórsson, 1985) is based on the relationship between silica and total carbonate concentrations in hot spring discharges to estimate subsurface temperatures. The model assumes that both aqueous silica and CO₂ concentrations are fixed by temperature dependent solute/mineral equilibrium in the reservoir, that most of the dissolved total carbonate is in the form of carbon dioxide, and temperature dependence of silica is controlled by quartz at temperatures above about 200°C. Boiling leads to instant degassing of CO₂, but increasing silica concentration, so boiling springs plot above the curve in Figure 10b, whereas mixed unboiled waters plot below the curve as both silica and carbonate concentrations decrease. The aquifer temperature is estimated to be 207°C by linear

extrapolation of the data points to the equilibrium curve. The samples are divided into three groups by this model: 1) Boiled and degassed waters above the curve; 2) Mixed waters below the curve; and 3) Steam-heated waters (samples 263 and 272) far away from the curve. This is consistent with the foregoing discussion (Section 4.2).

In the chloride-enthalpy mixing model (Fournier, 1979b) it is assumed that the concentrations of chloride in hot spring waters are fixed by boiling and mixing. The result obtained by this model for the Hveragerdi field is given in Figure 10c. In Figure 10c, the steam loss line is drawn by linking steam point (0 ppm Cl and 2778 kJ/kg enthalpy) and well discharge point with the highest chloride concentration (Well 7); line a is drawn radiating from the average enthalpy and chloride concentration point of three cold springs with temperatures of less than 10°C in the area to the point of the boiling spring 262 with the lowest chloride concentration except for the above-mentioned two steam-heated waters. Line a is the mixing line that is the upper boundary for all of the estimated points except for the two noted above. The intersection point of the steam loss line and line a indicates an original hot water temperature of 260°C. Line b sets a lower limit for the waters that seem to be mixed water. The temperature predicted from line b is 132°C.

4.5 Gas chemistry and subsurface temperature estimation

4.5.1 Gas chemistry of steam

During the last 15 years, many fumarole steam samples have been collected in the Hveragerdi area (Figure 1). The gas composition of some of these fumarole steam samples is presented in Table 5.

The concentrations of CO₂, H₂S, H₂ and N₂ in fumarole steam of this field are in the range 48.3-161.9, 0.33-8.91, 0.07-9.38 and 0.26-26.2 mmoles/kg steam, respectively. CH₄, Ar and O₂ are generally less than 1% of the total gas. Gaseous compounds make up only about 0.02% of the total volume of the fumarole steam, considerably less than observed in most other high-temperature geothermal fields in Iceland. The gas chemistry of this field is also characterised by low concentrations of H₂S and H₂ compared to the neighbouring fields of Nesjavellir and Hengladalir (Ármansson et al., 1986; Arnórsson, 1986).

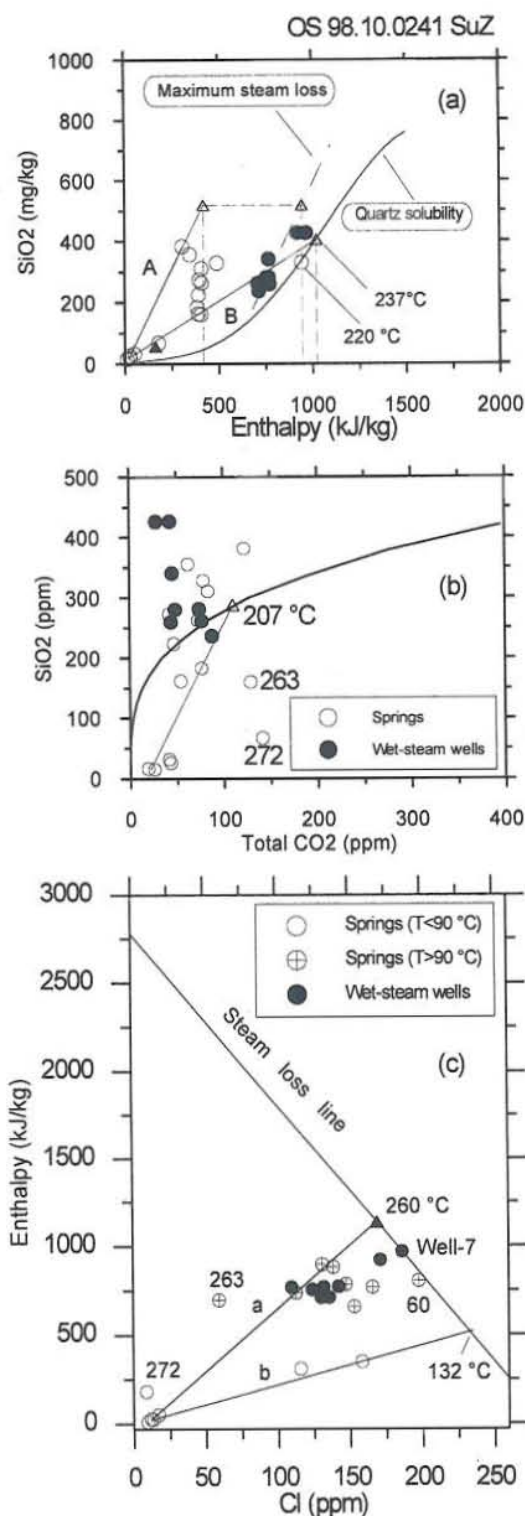


FIGURE 10: Results for subsurface temperatures evaluated by a) the silica-enthalpy model; b) the carbonate-silica model; and c) the chloride-enthalpy model in the Hveragerdi geothermal field

the neighbouring fields of Nesjavellir and Hengladalir (Ármansson et al., 1986; Arnórsson, 1986).

TABLE 5: Gas composition of fumarole steam in the Hveragerdi area (in mmoles/kg steam); data for samples no. 264-267 from Gestsdóttir and Geirsson (1990); no.28-69 from Arnórsson and Gunnlaugsson (1985); and no. G62-G71 from Ívarsson (1996)

Sample no.	CO ₂	H ₂ S	H ₂	CH ₄	N ₂	Ar	O ₂
264	66	0.6	0.26	0.006	2.08	0.037	0.09
265	98.4	0.33	1.87	0.057	3.08	0.052	0.15
266	125.3	3.32	2.93	0.059	3.13	0.056	0.14
267	133.7	8.68	8.54	0.143	6.14	0.108	0.2
268	119.8	7.23	5.51	0.149	5.29	0.095	0.13
269	99.5	1.97	1.91	0.035	2.73	0.045	0.14
270	113.2	8.91	4.43	0.118	4	0.066	0.19
271	136.3	8.32	4.66	0.096	4.08	0.067	0.3
273	132.1	6.71	1.1	0.114	5.8	0.099	0.23
276	67.8	2.67	0.07	0.004	2.63	0.035	0.11
28	107.1	5.1	3.96	0.161	11.14	0.365	0.29
30	108.6	7.33	3.1	0.174	3.87	0.163	0
31	140.3	8.37	9.38	0.168	8.87	0.273	0.06
32	128.1	1.43	5.46	0.158	6.5	0.247	0.02
37	58.9	2.92	0.07	nd	4.67	0.132	0.7
41	151.4	8.91	8.32	0.196	5.28	0.279	0
42	161.9	2.9	2.34	nd	26.2	0.994	4.74
43	141.1	1.14	3.12	0.076	2.24	0.052	0
64	94.5	4.66	3.67	0.09	2.34	0.049	0.09
65	83.9	3.47	3.06	0.488	1.9	0.04	0.14
66	99.6	4.2	2.94	0.038	1.7	0.043	0.21
67	77.9	3.74	0.34	0.058	2.82	0.07	0.1
68	48.3	2.36	0.39	0.019	1.45	0.048	0.06
69	67.1	2.68	0.37	0.055	8.65	0.171	0.77
						Ar+O ₂	
G62	64.15	2.8	nd	nd	nd	nd	
G63	100.43	5.68	4.2	0.193	6.555	0.223	
G69	123.984	6.32	1.043	0.197	0.261	0.014	
G70	124.553	6.38	0.97	0.16	4.595	0.169	
G71	93.778	4.13	0.47	0.016	2.046	0.27	

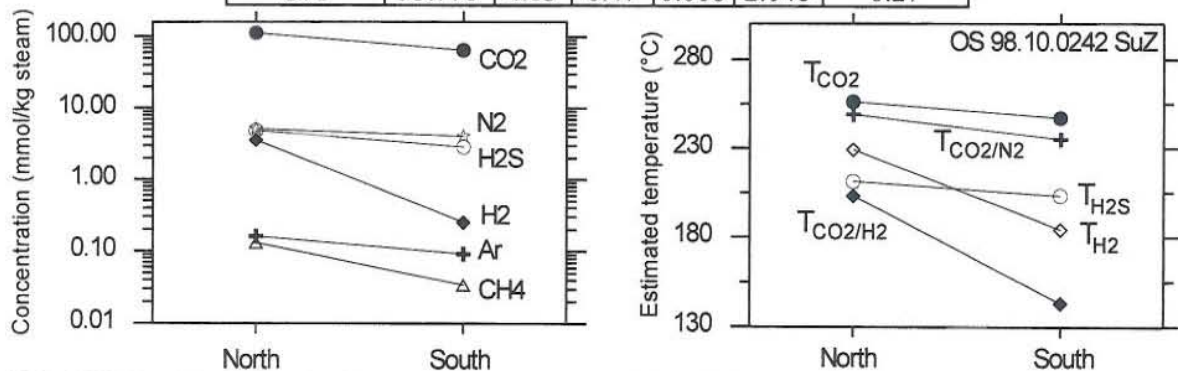


FIGURE 11: Variations in a) gas concentrations; and b) gas geothermometry results for Hveragerdi

If a line is drawn arbitrarily from east to west through well G3 (Figure 1), the geothermal field can be divided into a northern part and a southern part. For each part, the average gas composition is shown in Figure 11a. The concentrations of CO₂, H₂S, H₂, CH₄, N₂ and Ar decrease significantly from north to south in this field. H₂S, H₂, CH₄ and CO₂ concentrations change relatively more than those of N₂ and

Ar owing to the former being more reactive. It is also noted that samples collected at higher altitudes in the ridges between the valleys contain less H_2 and H_2S than samples collected on the valley floors, most likely due to oxidation of these reduced species above groundwater level.

4.5.2 Gas geothermometry results

As discussed in Section 3.2, the concentrations of various gases in fumarole steam and steam from wet-steam wells are considered to be in equilibrium with mineral buffers at any given temperature. Five gas geothermometers listed there are used for this report. Results are presented in Table 6. The results for

TABLE 6: Results of gas geothermometry ($^{\circ}C$) of fumaroles and wet-steam wells for Hveragerdi

Type	Sample no.	T_{CO_2}	T_{H_2S}	T_{H_2}	T_{CO_2/H_2}	T_{CO_2/N_2}
Fumarole	264	249	159	190	151	251
Fumarole	265	263	142	223	197	251
Fumarole	266	270	207	230	203	258
Fumarole	267	272	234	248	232	240
Fumarole	268	269	229	241	222	241
Fumarole	269	263	192	223	197	255
Fumarole	270	267	235	237	218	247
Fumarole	271	273	233	238	214	252
Fumarole	273	272	227	214	173	241
Fumarole	276	250	201	168	112	245
Fumarole	28	265	219	235	216	215
Fumarole	30	266	229	231	209	247
Fumarole	31	274	233	250	233	230
Fumarole	32	271	183	241	220	237
Fumarole	37	244	203	168	117	223
Fumarole	41	276	235	248	228	248
Fumarole	42	278	203	226	189	202
Fumarole	43	274	177	231	201	271
Fumarole	46	261	217	234	218	258
Fumarole	65	257	208	231	216	260
Fumarole	66	263	214	230	210	269
Fumarole	67	255	210	194	154	247
Fumarole	68	237	197	196	172	252
Fumarole	69	249	201	196	161	209
Fumarole	G62	248	202			
Fumarole	G63	263	222	236	220	229
Fumarole	G69	270	225	213	173	323
Fumarole	G70	270	226	212	171	246
Fumarole	G71	261	213	200	158	261
Well	G2	220	215	206	201	347
Well	G4	239	210	216	203	229
Well	G6	243	201	218	204	175
Well	G7	251	224	216	196	185
Well	NLFI-1	243	225	216	202	229
Well	NLFI-2	257	224	216	190	237
Well	H-1	248	220	218	201	
Well	H-2	248	226	223	208	

fumaroles indicate that the subsurface temperatures calculated by these gas geothermometers decrease from the northern to the southern part of the geothermal field. This is well demonstrated in Figure 11b. The CO_2 -geothermometer gives the highest temperature values, an average of 256°C for the north, and 247°C for the south. The H_2S -geothermometer indicates aquifer temperature of 211°C for the north, and 203°C for the south. The H_2 -geothermometer gives an average subsurface temperature of 229°C for the north, and 184°C for the south, which agrees excellently with the measured temperatures in wet-steam wells. In this field, the measured temperatures range from 215 to 230°C for the northern part, and from 167 to 198°C for the southern part. The CO_2/H_2 -geothermometer gives the lowest subsurface temperature values, an average of 203°C for the north, and 143°C for the south. The CO_2/N_2 -geothermometer gives 249°C for the north and 235°C for the south.

For data from wells, the CO_2 -, the H_2S - and the H_2 -geothermometers give an average subsurface temperature of 247°C for the north and 246°C for the south, 213°C for the north and 220°C for the south, and 217°C for the north and 216°C for the south, respectively. The CO_2/H_2 -geothermometer indicates an average subsurface temperature of around 200°C both for the north and the south. The CO_2/N_2 -geothermometer gives an average subsurface temperature of 180°C for the north and 259°C for the south, which is not reliable due to the danger of even a small proportion of air drawn in during upflow or sampling causing significant interference.

The discrepancy between the estimated subsurface temperatures obtained by various gas geothermometers may be explained by various causes. One is that it is a relatively old geothermal area which means that the geothermal system has cooled down, and such a system tends to be high in CO_2 and yield high CO_2 geothermometer temperatures. For the high CO_2 concentration in such systems, various explanations have been offered, one being that there is probably a steady flow of CO_2 from the magma which becomes masked in the high concentrations in new systems, but with lowered equilibrium concentrations along with a reduced steam fraction, the CO_2 concentration of the steam may become significantly higher than the equilibrium concentration. As speculated by Arnórsson and Gunnlaugsson (1985) and Zhao and Ármannsson (1996), different mineral buffers may control H_2S and H_2 concentrations at different temperatures. The good results obtained by the H_2 - gas geothermometer is probably due to better defined buffers for H_2 than for others. Another explanation may be the combination of condensation and oxidation in the upflow. The low H_2S temperatures are due to loss of H_2S by oxidation, especially for the samples collected on high ground. The higher CO_2 temperatures are partially caused by condensation which leads to a higher CO_2 concentration in the steam which is reflected in data from wells in whose fluid the CO_2 concentrations are lower than those of the nearby fumarole steam. The CO_2/H_2 - geothermometry temperatures are not reliable probably because of inflow of CO_2 from depth and/or due to complex effects of condensation and oxidation.

By integration of solute geothermometry results, mixing model studies and the above discussed gas geothermometry results, the maximum subsurface temperatures of the Hveragerdi high-temperature geothermal system may be considered to be about 240 - 260°C .

4.6 Summary

In the Hveragerdi high-temperature geothermal field, solute-mineral equilibrium studies suggest that geothermal fluids accessed by boreholes are close to equilibrium with hydrothermal alteration minerals, but boiling/degassing and mixing in up-flow zones lead to a shift from subsurface equilibrium conditions for thermal waters emerging in hot springs. The solute geothermometers and the $\log(Q/K)$ method give reasonable estimated subsurface temperatures for well discharges, but their use for hot spring waters is limited by boiling/degassing and mixing processes in the upflow.

The mixing and boiling/degassing effects have been detected, and eliminated by three mixing models. The original hot water temperatures are estimated to be about 210 - 260°C which compares quite well with measured temperatures in wells, the solute geothermometer temperatures or well discharges, and the gas geothermometer temperatures or fumarole steam and steam from wet-steam wells.

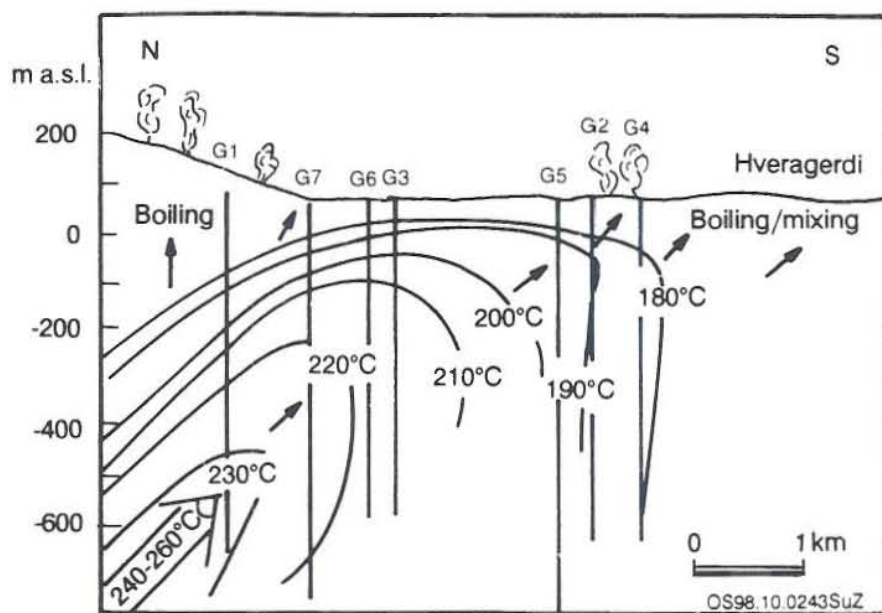


FIGURE 12: A conceptual model of the Hveragerdi high-temperature geothermal field, isothermal lines based on temperature logging data in wells, and the temperatures of deep geothermal waters derived from gas geothermometers and mixing model results; revised from Geirsson and Arnórsson (1995)

By combination of hydrochemical and gas chemical studies with temperature logging data in boreholes, a conceptual model for the Hveragerdi high-temperature geothermal field can be constructed and the result is presented in Figure 12. Geothermal fluids of the Hveragerdi geothermal field come from north and flow towards south along with the temperature decrease caused by mixing processes with cold groundwaters as well as conductive cooling. Boiling/degassing occurs in the up-flow zones.

5. SELECTED HOT SPRINGS, JIANGXI PROVINCE, SE-CHINA

5.1 General background

Jiangxi province, SE-China, is one of the provinces in which hot springs are most widely distributed in China. In this province, 96 hot springs with temperatures ranging from 25 to 88°C have been found. Systematic compilations of hot springs in the region were carried out by Li (1979) and Sun (1988).

Two hot spring areas in the Province close to Linchuan City in which the East China Geological Institute is located, the Maanping hot spring area and the Linchuan hot spring area, have been selected for this study. The locations are shown in Figure 13. In the Linchuan hot

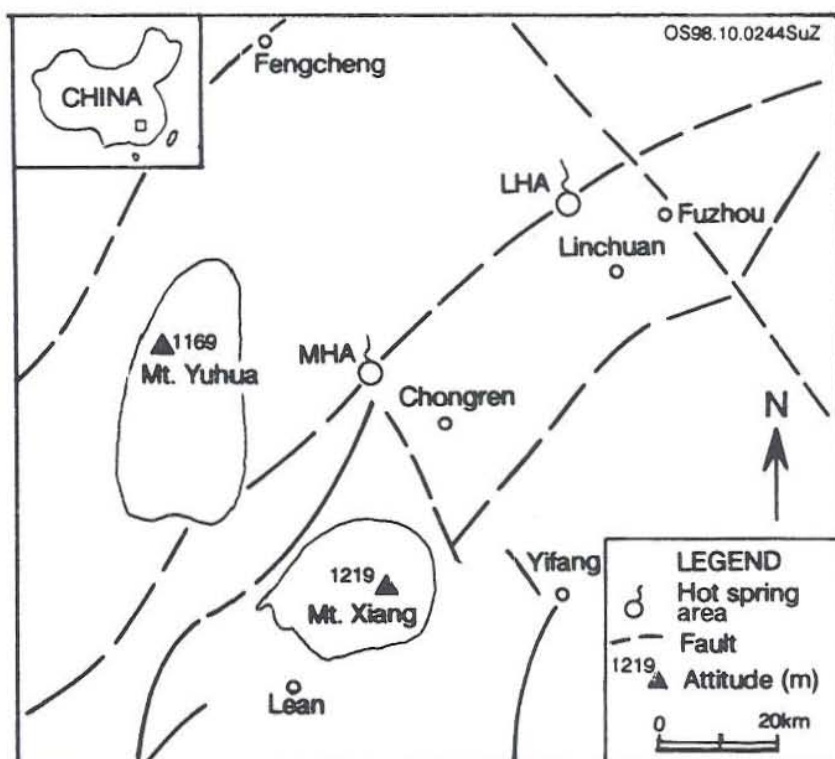


FIGURE 13: Location of the Maanping hot spring area (MHA) and the Linchuan hot spring area (LHA)

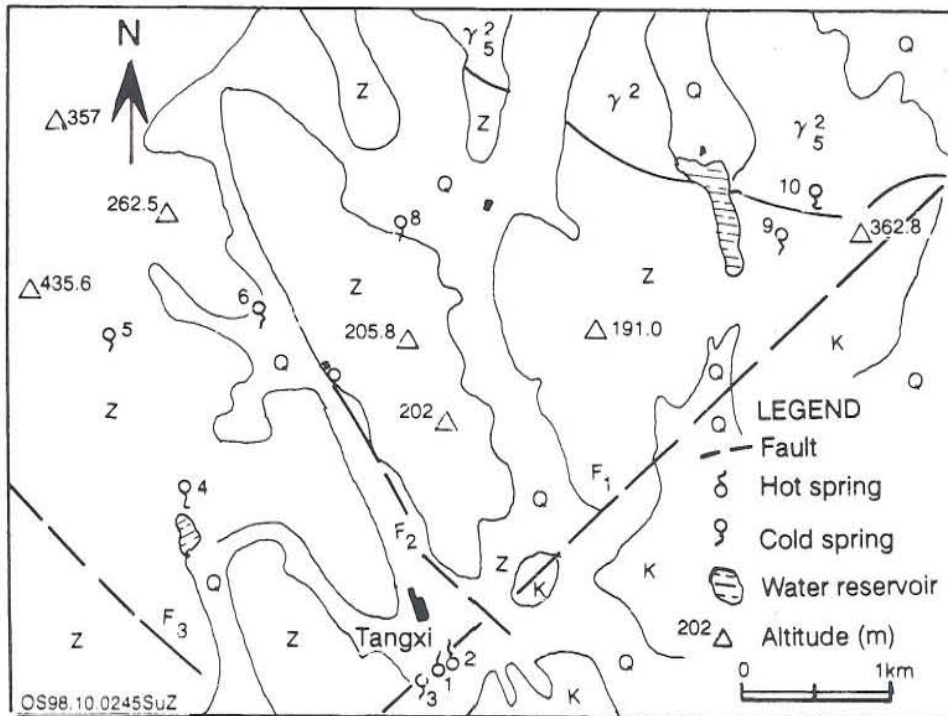


FIGURE 14: Geological map of the Maanping hot spring area, numbers at springs refer to sampling locations

spring area, one hot spring sanatorium has been in operation for more than 20 years, and is famous all over the province for its slightly radioactive bicarbonate water which is used as a treatment for rheumatism, arthritis, neurosis and various skin diseases such as psoriasis and scabies.

Geologically, the two areas are quite similar to each other (Figures 14 and 15). Strata exposed in the two areas include the Sinian system (Z) composed of schists, the Cretaceous system (K) characterised by

sandstone and conglomerate, and the Yanshanian granite (γ_5^2) as well as Quaternary sediments (Q). In addition, carboniferous sandstone (C) is widely distributed in the Linchuan Hot Spring area.

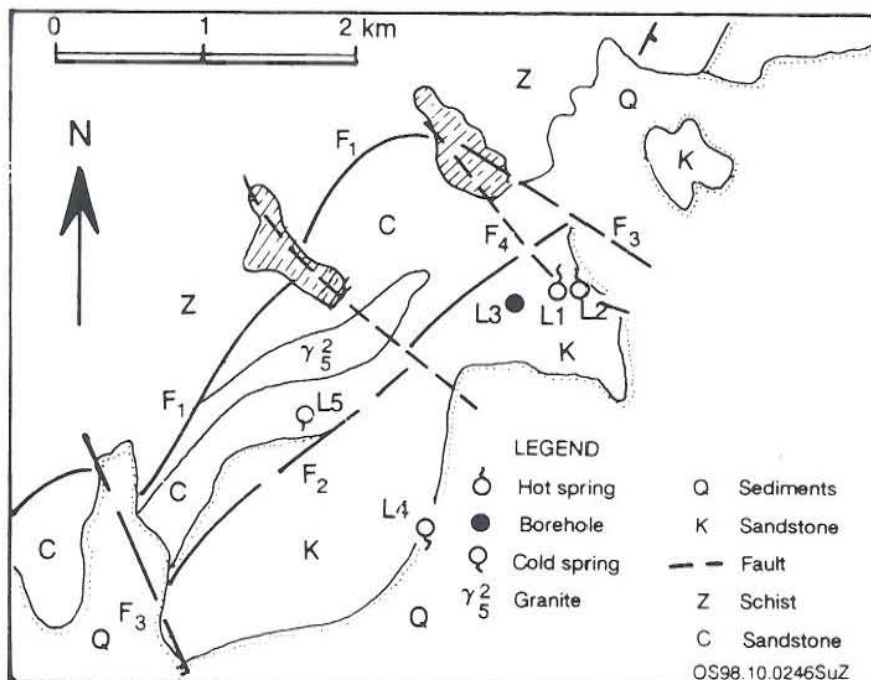


FIGURE 15: Geological map of the Linchuan hot spring area, L numbers refer to sampling locations

The hydrochemical and isotopic composition of natural waters in the two areas was studied in the late 1980's and early 1990's (Sun, 1988; Sun et al., 1992; Li et al., 1993). The analytical data are presented in Table 7, sampling locations are in Figures 14 and 15.

TABLE 7: Chemical and isotopic composition of spring waters from Jiangxi Province, SE-China (concentrations in ppm)

No.	T (°C)	pH/°C	SiO ₂	Fe	Na	K	Ca	Mg	CO ₂	SO ₄	H ₂ S	Cl	F	δD‰	δ ¹⁸ O‰	³ H (T.U)	Ra (Bq/l)	Rn (Bq/l)
1	42	6.13/20	60	0.56	218.3	24.2	109	4.88	1553.5	30	1.13	9.23	4.04	-44.1	-7.23	10	0.685	20.4
2	41	6.19/20	50	1.14	208.3	36.8	96.4	9.9	1453.5	30	1.36	8.88	3.13	-45.4	-6.84	7.5	0.892	0.892
3	20	5.97/20	25	nd	2	2.5	1.5	0.61	7.91	1.4	nd	0.25	nd	-34.3	-5.46	33.3	nd	nd
4	18	5.8/20	16	nd	0.2	0.3	4	2.1	16.95	0.15	nd	0.2	nd	-36.9	-5.7	nd	nd	nd
5	18	5.9/20	10	nd	1.7	2.9	1.2	0.2	11.04	0.05	nd	0.5	nd	-37.4	-5.93	nd	nd	nd
6	19	6.4/20	14	nd	0.4	0.6	8	4	33.04	0.1	nd	0.5	nd	-29.8	-5.15	nd	nd	nd
7	22	6.1/20	14	nd	0.1	0.2	10.8	4.9	41.33	0.05	nd	0.6	nd	-35.4	-5.6	39.7	nd	nd
8	20	6.8/20	16	nd	2	4.3	3	0.4	18.03	0.5	nd	0.4	nd	-42.3	-6.3	32.9	nd	nd
9	19	5.6/20	12	nd	1.3	2.4	1.6	1.8	14.28	1.5	nd	0.6	nd	-35.8	5.57	nd	nd	nd
10	20	6.5/20	20	nd	2	3.1	2.3	1.8	19.9	1	nd	0.6	nd	-35.6	-5.78	43.6	nd	nd
L1	41	7.55/20	70	nd	4.3	3.4	33	3.12	97.9	17.04	nd	2.19	4	-49	-6.7	nd	2.553	52.15
L2	39	7.4/20	60	nd	2.9	3.9	48.1	4.87	87.3	33.62	nd	6.68	3.5	-38.4	-6.57	nd	nd	nd
L3	59	8.27/20	80	nd	13.5	15.5	61.1	2.19	93.1	72	nd	2.49	6	-52	-6.8	nd	nd	nd
L4	19	6.99/20	30	nd	1	1.9	1.6	0.62	6.69	2.98	nd	1.63	nd	-31.7	-5.66	nd	nd	nd
L5	18	5.89/20	18	nd	2.2	2.5	1	0.25	8.88	1.25	nd	1.63	nd	-36.2	-6.13	nd	nd	nd

nd: not determined.

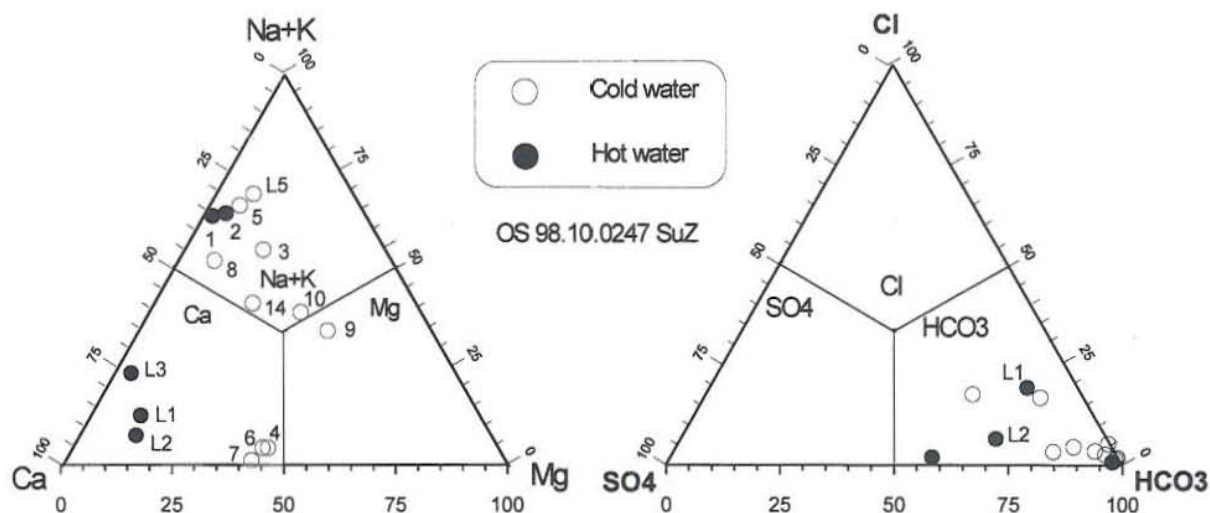


FIGURE 16: Triangular diagrams of relative component concentrations, in equivalents, for the Maanping and Linchuan waters

5.2 Water chemistry

All the data are plotted in the triangular diagram (Figure 16) as relative concentrations. The waters in the two areas can be classified into three types: 1) Mg-HCO₃ type, includes one cold water sample no. 9; 2) Ca-HCO₃ type, includes cold water samples no. 4, 6 and 7 and hot water samples no. L1, L2, L3; 3) Na+K-HCO₃ type, the rest of the samples. Clearly, the difference in the chemical composition of hot spring water in the two areas is quite significant.

All the data points were plotted in Giggenbach's Na-K-Mg triangular diagram (Figure 17). It shows that all the waters in the two areas are immature ones for which the application of cation geothermometers is not suitable. Linear relations seem to exist between Cl and δ¹⁸O, SiO₂, K and Na concentrations (Figure 18) which may indicate some sort of mixing of hot spring water with cold groundwater. However, the relationship is not necessarily due to direct mixing of two end members.

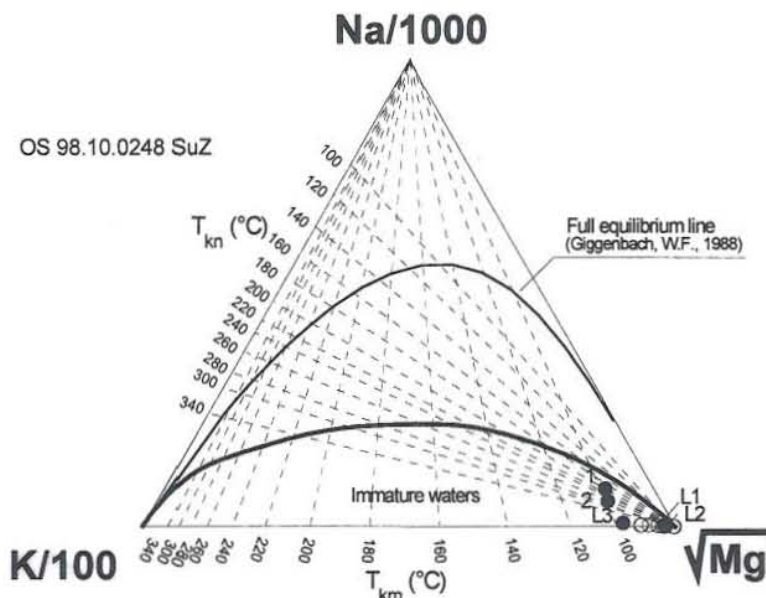


FIGURE 17: Na-K-Mg triangular diagram for the Maanping and the Linchuan waters

5.3 Isotope geochemistry of natural waters

In the region, the local meteoric water line is (Sun et al., 1992):

$$\delta D = 8.4\delta^{18}O + 11.8 \tag{11}$$

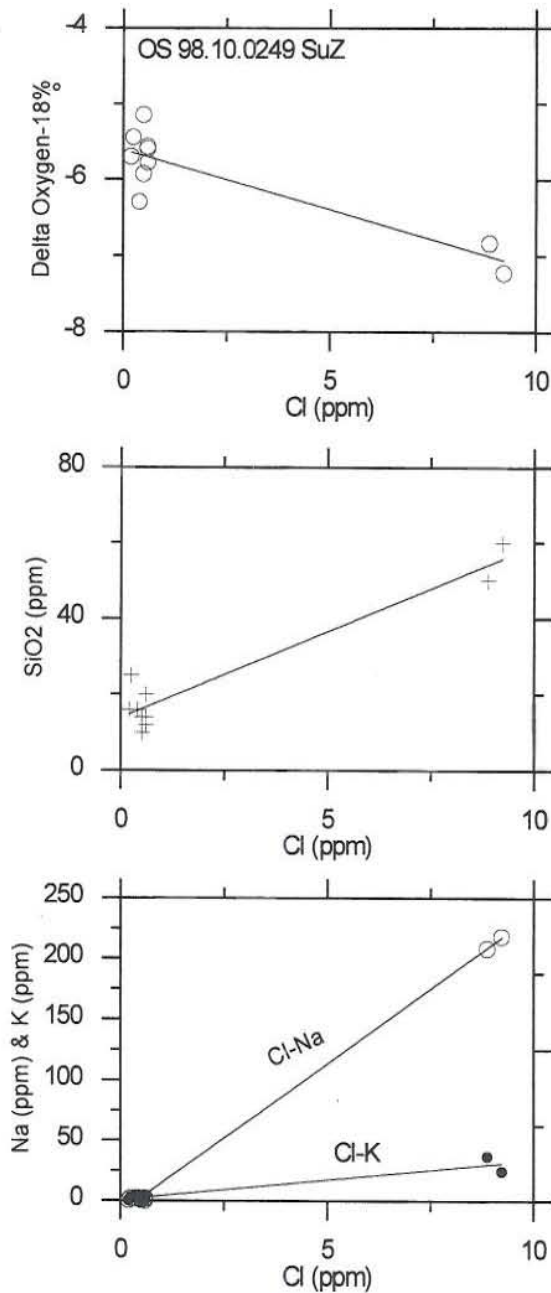


FIGURE 18: The correlations between Cl and $\delta^{18}O$, SiO_2 , K and Na of the Maanping and Linchuan waters

The concentrations of radium and radon in hot spring waters in the two areas were measured and used to estimate the age of the hot spring water using the following dating equation (Cherdynstsev, 1969):

$$t = -\frac{1}{\lambda} \ln\left(1 - \frac{N_{Ra}}{N_{Rn}}\right) \quad (14)$$

where, t is the age of water in years, λ is the decay constant of radium ($4.33 \cdot 10^{-4}$); N_{Ra} and N_{Rn} are the radium and radon concentrations of the water respectively. The estimated age of the thermal water is about 80 years for the Maanping hot springs, and 120 years for the Linchuan hot springs.

which is similar to the world meteoric line (WML)(Craig, 1961). The δD and $\delta^{18}O$ values for thermal waters in the two hot spring areas are roughly in line with the local meteoric water line (Figure 19), which indicates that the thermal waters are of meteoric origin. No oxygen shift is found showing that either the subsurface temperature of the geothermal reservoirs in the two areas are quite low and the thermal waters belong to low-enthalpy geothermal resources or the water/rock ratio is quite high in the systems.

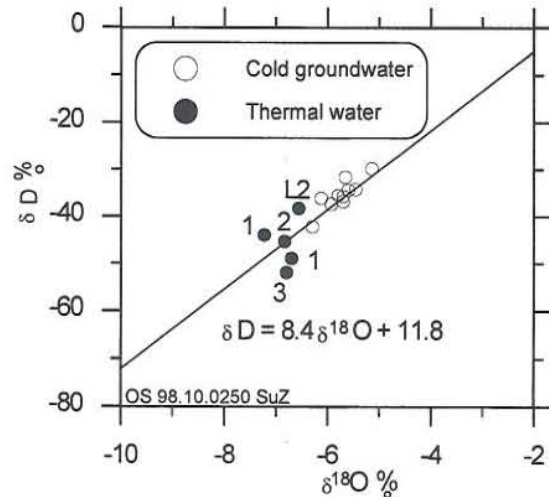


FIGURE 19: The δD vs $\delta^{18}O$ plot for natural waters in the Maanping and Linchuan areas

In the region, the correlation lines between altitude and isotopic composition of the mean precipitation are as follows (Li et al., 1993):

$$\delta D = -27.6 - 0.031H \quad (12)$$

$$\delta^{18}O = -4.82 - 0.0033H \quad (13)$$

where, δD and $\delta^{18}O$ values are expressed in ‰ (SMOW) and H is altitude (m). According to the equations, the average altitude of the recharge area for the hot springs was estimated to be about 600 m.

Hydrogeological investigations (Li, 1979; Sun, 1988) showed that the recharge areas for the Maanping and Linchuan hot springs are probably the region located 15-20 km northwest of the Maanping hot spring area at an altitude of about 500-700 m, and the region located around 20-25 km northwest of the Linchuan hot spring area at an altitude of about 500-800 m, respectively. By comparing the estimated hydraulic conductivity, about $4-7 \times 10^{-6}$ m/s (Sun, 1988), for the representative rocks in the two areas with the recharge distances, the estimated ages of the spring waters in these areas seem to be reasonable.

5.4 Subsurface temperature estimation

5.4.1 Solute geothermometry results

As discussed above, all the thermal waters in the two areas are immature waters, so cation geothermometers such as Na-K and Na-K-Ca geothermometers are not applicable for these hot waters. The only option is to use silica geothermometers. The results are given in Table 8.

TABLE 8: Silica geothermometry results of the Maanping and Linchuan thermal waters

Sample no.	T_{mea} (°C)	T_{quartz} (°C)	$T_{\text{chalced-1}}$ (°C)	$T_{\text{chalced-2}}$ (°C)
1	42	111	81	82
2	41	102	72	73
3	41	118	90	90
4	39	111	81	82
5	59	124	97	97

T_{quartz} and $T_{\text{chalced-1}}$ equations according to Section 3.1;
 $T_{\text{chalced-2}}$ equation from Arnórsson et al. (1983b).

Clearly, the estimated subsurface temperatures range from 72 to 124°C for the two hot spring areas. Results of drilling show that the temperature of thermal waters from wells above 1000 m depth is not higher than 100°C in the province (Lin, pers. comm.). So the chalcedony geothermometer temperatures, which are about 70-100°C, are probably closer to the reservoir temperature than the quartz temperatures.

5.4.2 Log(Q/K) diagrams

The log(Q/K) values at varying temperatures calculated in the same way as for the Hveragerdi waters using SOLVEQ, and the log(Q/K) vs. temperature diagrams, for the Maanping and Linchuan thermal waters are shown in Figure 20. The equilibrium temperatures for selected minerals range from approximately 40 to 100°C for the Maanping thermal waters, and from 38 to 120°C for the Linchuan thermal waters. For the Maanping hot springs, it can be seen that chalcedony, calcite, aragonite and dolomite cross the zero line of log(Q/K) within the range 60-80°C, which indicates that these minerals are close to equilibrium with the solution in the system. For the Linchuan hot springs, calcite, aragonite and dolomite seem to be in equilibrium with the solution at discharge temperatures. The log(Q/K) diagram for the hot water from a borehole, sample No. L3, shows that carbonate minerals are supersaturated and this suggests a degassing effect. No cluster can be found for any of the diagrams in Figure 20 probably due to mixing, and/or degassing, as well as incomplete chemical analyses that do not include Al and Fe concentrations and, thus, only relatively few minerals can be studied.

5.5 Evaluation and elimination of mixing effects

In the two areas, the measured temperatures of thermal waters are 30-40°C lower than the chalcedony geothermometer temperatures, the linear relationships between Cl and $\delta^{18}\text{O}$, SiO_2 , K and Na in natural

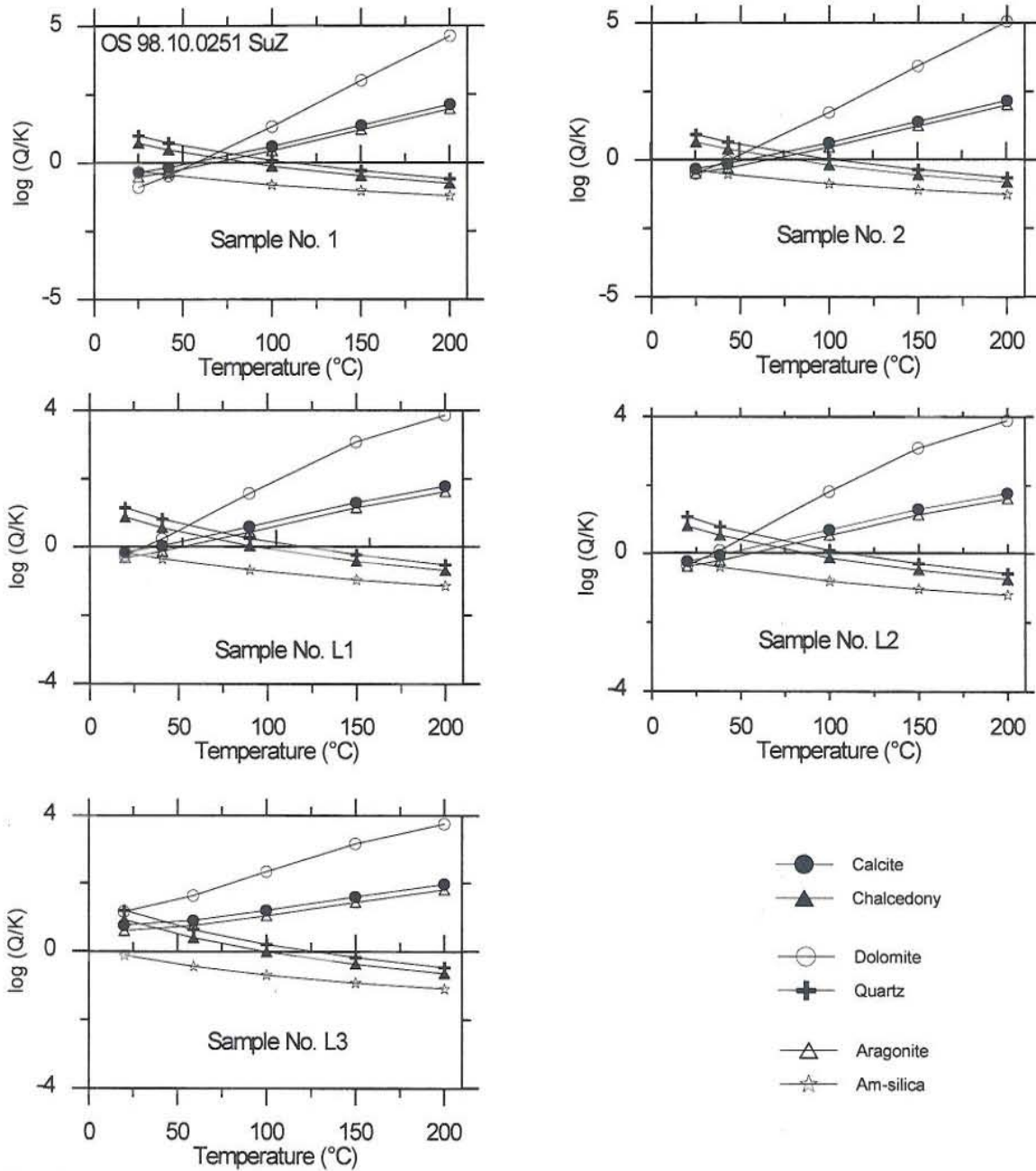


FIGURE 20: Log(Q/K) vs. temperature diagrams for the Maanping and Linchuan thermal waters

waters discussed in Section 5.2 may exist, and the tritium concentrations of the thermal waters are in contradiction with the ages dated by the radium/radon method. Such evidence implies that the thermal waters in the two areas may contain water of mixed origin.

In order to eliminate such mixing effects, the silica-enthalpy mixing model (Truesdell and Fournier, 1977) was used (Figure 21). It gives the improbably high temperature of 166°C for the hot waters. The reason for this is that conductive cooling probably took place during the upflow of the thermal waters. The mixing model is not applicable in such cases.

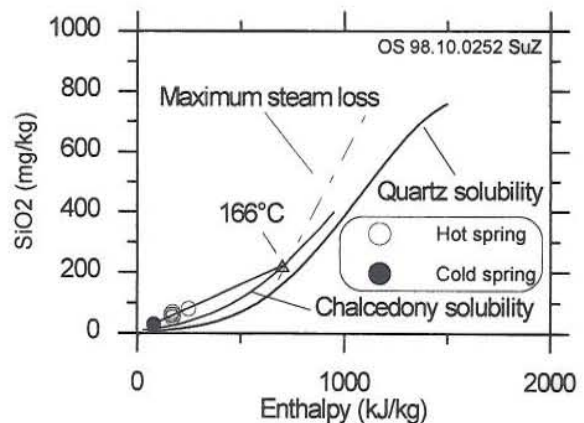


FIGURE 21: The silica-enthalpy mixing model for the Maanping and the Linchuan hot springs

As is well known, unmixed thermal waters recharged before the thermonuclear tests of 1950's should be tritium-free. If we take the average tritium content of cold waters in Table 7 as that of the cold water component in the mixed water, and the content of the hot spring waters as that of the mixed water, then the approximate fraction of cold water in the mixed water can be estimated by the following equations:

$$X + Y = 1 \quad (15)$$

$$T_h \cdot X + T_c \cdot Y = T_m \cdot (X + Y) \quad (16)$$

where X is the fraction of unmixed hot water, Y is the fraction of cold water, and T_h , T_c and T_m are tritium concentrations of unmixed hot water, cold water and mixed water, respectively.

If we put the average tritium concentration of cold water, 37 T.U., and the tritium concentration, 7.5 T.U and 10 T.U for hot springs numbered 1 and 2, respectively, into the above equations, the cold water fraction is estimated to be about 20-30%. If some low-tritium cold water possibly involved in the mixing process is taken into account, the fraction of cold water would be higher than the above estimated values.

5.6 Summary

Thermal waters of the Linchuan hot spring area are of the Ca-HCO₃ type, and those of the Maanping hot spring area are of the Na-K-HCO₃ type. In the two areas, thermal waters were recharged before the thermonuclear tests by local meteoric water in the recharge area at an altitude of about 600 m. For the Maanping low-temperature system, the chalcedony geothermometer gives subsurface temperatures of about 70-80°C which compare well with the equilibrium temperatures of 60-80°C for carbonate minerals from log(Q/K) diagrams. For the Linchuan hot spring area, the chalcedony geothermometer yields subsurface temperatures of about 80-100°C. In such a case, the log(Q/K) method can be used to identify equilibrium state of minerals with the solution, although it is difficult to determine the subsurface temperatures by the method because of possible mixing, and/or degassing, as well as the absence of Al and Fe analyses. The mixing process can be evaluated using a tritium concentration but the silica-enthalpy mixing model may not be applicable for the case because of conductive cooling.

6. CONCLUSIONS AND DISCUSSION

An overall equilibrium between fluid and hydrothermal minerals is attained or nearly attained for geothermal fluids from wells in the Hveragerdi high-temperature field, SW-Iceland. In such cases, the solute geothermometers and the log(Q/K) method yield estimated temperatures that compare well with measured aquifer temperatures. Boiling/degassing and mixing in upflow zones lead to deviation from equilibrium for hot spring fluids and difficulties in applying solute geothermometers and the log(Q/K) method to estimate subsurface temperatures. Three mixing models can deal with such difficulties

The H₂-gas geothermometer gives more reasonable results than the CO₂/H₂-, H₂S-, and CO₂-geothermometers, probably due to its better defined buffers. The CO₂/N₂-geothermometer may not be reliable owing to the danger of even a small proportion of air drawn in during upflow or sampling causing considerable interference.

In the Maanping and the Linchuan low-temperature geothermal systems, an overall equilibrium of mineral-solution is not attained but some secondary carbonate minerals seem to approach equilibrium with the solution. Cation geothermometers are not applicable in such cases, while the chalcedony geothermometer is suggested as the most likely useful tool to estimate subsurface temperatures of such systems. Applying either geothermometers or mixing models in geothermal studies, the fundamental assumptions should be carefully considered, otherwise erroneous results can easily be obtained.

ACKNOWLEDGEMENTS

I would like to express my gratitude to Dr. Ingvar B. Fridleifsson, director of the UNU Geothermal Training Programme, for the fellowship award and his excellent guidance, Mr. Lúdvík S. Georgsson and Ms. Guðrún Bjarnadóttir for their efficient help and kindness in my daily life and work. Special thanks are due to Dr. Halldór Ármannsson, my advisor, for sharing his experience and critical advice during all stages of my preparation of this report. I am very grateful to Prof. Stefán Arnórsson, University of Iceland, for his excellent lectures on chemical thermodynamics and for his kind provision of some unpublished data. Many thanks are due to the Orkustofnun staff members who are too many to name here, for their kindest help during my stay in Iceland. I would like to extend my appreciation to Prof. Wang Ji-yang, Chinese Academy of Sciences, and Prof. Li Xueli, East China Geological Institute, for their recommendations and encouragement.

REFERENCES

- Ármannsson, H., 1989: Predicting calcite deposition in Krafla boreholes. *Geothermics*, 18, 25-32.
- Ármannsson, H., Benjamínsson, J., and Jeffrey, A.W.A., 1989: Gas changes in the Krafla geothermal system, Iceland. *Geochemical Geology*, 76, 175-196.
- Ármannsson, H., Gíslason, G., and Torfason, H., 1986: Surface exploration of the Theistareykir high-temperature geothermal area, with special reference to the application of geochemical methods. *Applied Geochemistry*, 1, 47-64.
- Arnórsson, S., 1985: The use of mixing models and chemical geothermometers for estimating underground temperature in geothermal systems. *J. Volc. Geotherm. Res.*, 23, 299-335.
- Arnórsson, S., 1986: Chemistry of gases associated with geothermal activity and volcanism in Iceland. A review. *J. Geophys. Res.*, 91, 12261-12268.
- Arnórsson, S., 1991: Geochemistry and geothermal resources in Iceland, In: D'Amore, F. (co-ordinator), *Applications of geochemistry in geothermal reservoir development*. UNITAR/UNDP publication, Rome, 145-196.
- Arnórsson, S., and Gunnlaugsson, E., 1985: New gas geothermometers for geothermal exploration - calibration and application. *Geochim. Cosmochim. Acta*, 49, 1307-1325.
- Arnórsson, S., Gunnlaugsson, E., and Svavarsson, H., 1983a: The chemistry of geothermal waters in Iceland II. Mineral equilibria and independent variables controlling water compositions. *Geochim. Cosmochim. Acta*, 47, 547-566.
- Arnórsson, S., Gunnlaugsson, E., and Svavarsson, H., 1983b: The chemistry of geothermal waters in Iceland III. Chemical geothermometry in geothermal investigations. *Geochim. Cosmochim. Acta*, 47, 567-577.
- Arnórsson, S., Sigurdsson, S. and Svavarsson, H., 1982: The chemistry of geothermal waters in Iceland I. Calculation of aqueous speciation from 0°C to 370°C. *Geochim. Cosmochim. Acta*, 46, 1513-1532.
- Arnórsson, S., and Svavarsson, H., 1985: Application of chemical geothermometry to geothermal exploration and development. *Geoth. Res. Council, Transactions*, 9-1, 293-298.
- Bjarnason, J.Ö., 1994: *The speciation program WATCH, version 2.1*. Orkustofnun, Reykjavík, 7 pp.

- Cherdyntsev, V.V., 1969: *Uranium-234*. Moscow, Atomizdat, 123 pp.
- Craig, H., 1961: Isotopic variation in meteoric waters. *Science*, 133, 1702-1703.
- D'Amore, F., 1991: Gas geochemistry as a link between geothermal exploration and exploitation. In: D'Amore, F. (coordinator), *Application of geochemistry in geothermal reservoir development*. UNITAR/UNDP publication, Rome, 93-117.
- Fournier, R.O., 1977: Chemical geothermometers and mixing model for geothermal systems. *Geothermics*, 5, 41-50.
- Fournier, R.O., 1979a: A revised equation for Na-K geothermometer. *Geoth. Res. Council, Transactionns*, 3, 221-224.
- Fournier, R.O., 1979b: Geochemical and hydrologic considerations and the use of enthalpy-chloride diagrams in the prediction of underground conditions in hot spring systems. *J. Volc. & Geoth. Res.*, 5, 1-6.
- Fournier, R.O., and Potter, R.W. II, 1979: Magnesium correction to the Na-K-Ca chemical geothermometer. *Geochim. Cosmochim. Acta*, 43, 1543-1550.
- Fournier, R.O., and Potter, R.W. II, 1982: A revised and expanded silica (quartz) geothermometer. *Geoth. Res. Council Bull.*, 11-10, 3-12.
- Fournier, R.O., and Rowe, J.J., 1966: Estimation of underground temperatures from the silica contents of water from hot springs and wet steam wells. *Am. J. Sci.*, 264, 685-697.
- Fournier, R.O., and Truesdell, A.H., 1973: An empirical Na-K-Ca geothermometer for natural waters. *Geochim. Cosmochim. Acta*, 37, 1255-1275.
- Fridleifsson, I.B., 1979: Geothermal activity in Iceland. *Jökull*, 29, 47-56.
- Geirsson, K., and Arnórsson, S., 1995: Conceptual model of the Hveragerdi geothermal reservoir based on chemical data. *Proceedings of the World Geothermal Congress 1995, Florence, Italy*, 2, 1251-1256.
- Gestsdóttir, K., and Geirsson, K., 1990: *Chemistry of thermal waters in the Hveragerdi geothermal field*. University of Iceland, Reykjavik, unpublished report (in Icelandic), 90 pp.
- Giggenbach, W.F., 1980: Geothermal gas equilibria. *Geochim. Cosmochim. Acta*, 44, 2021-2032.
- Giggenbach, W.F., 1988: Geothermal solute equilibria. Derivation of Na-K-Mg-Ca geoindicators. *Geochim. Cosmochim. Acta*, 52, 2749-2765.
- Giggenbach, W.F., 1991: Chemical techniques in geothermal exploration. In: D'Amore, F. (coordinator), *Application of geochemistry in geothermal reservoir development*. UNITAR/UNDP publication, Rome, 119-142.
- Ívarsson, G., 1996: *Geothermal gases in the Hengill region. Collection and analyses*. Reykjavik Heating Service, Reykjavik, report XXXX (in Icelandic), 45 pp.
- Li X.L., 1979: The relationship between distribution of thermal waters and uranium mineralization in Jiangxi. *Journal of East China Geological institute*, 2, 21-29.
- Li X.L., Shi W.J., Sun Z.X., Zhou W.B., and Zhang W.M., 1993: *An oxygen and hydrogen isotope study of thermal springs in Jiangxi Province, SE-China*. IAEA, report of research contract no.6447/RB, 25 pp.

- Marini, L., Cioni, R., and Guidi, M., 1998: Water chemistry of San Marcos area, Guatemala. *Geothermics*, 27, 331-360.
- Ólafsson, M., 1988: *Sampling methods for geothermal fluids and gases*. Orkustofnun, Reykjavík, report OS-88041/JHD-06, 17 pp.
- Paces, T. (editor), 1991: *Fluid sampling for geothermal prospecting*. UNITAR/UNDP publication, Rome, 93 pp.
- Pang Z., and Reed, M., 1998: Theoretical chemical thermometry on geothermal waters: problems and methods. *Geochim. Cosmochim. Acta*, 62, 1083-1091.
- Reed, M.H., and Spycher, N.F., 1984: Calculation of pH and mineral equilibria in hydrothermal water with application to geothermometry and studies of boiling and dilution. *Geochim. Cosmochim. Acta*, 48, 1479-1490.
- Sigvaldason, G.E., 1962: Epidote and related minerals in two deep geothermal drill holes, Reykjavik and Hveragerdi, Iceland. *U. S. Geological Survey, prof. papers*, 450-E, 77-79.
- Spycher, N.F., and Reed, M.H., 1989: *User's guide for SOLVEQ: A computer program for computing aqueous-minerals-gas equilibria (revised prelim.edition)*. University of Oregon, Eugene, OR, 37 pp.
- Sun Z.X., 1988: *The formation conditions of hot springs in Jiangxi Province, SE-China*. MSc. thesis of East China Geological Institute, 50 pp.
- Sun Z.X., Li X.L., and Shi W.J., 1992: Isotopic geochemistry of natural waters in Jiangxi Province, SE-China. *Journal of East China Geological Institute*, 15, 221-228.
- Tole, M.P., Ármannsson, H., Pang Z.-H., and Arnórsson, S., 1993: Fluid/mineral equilibrium calculations for geothermal fluids and chemical geothermometry. *Geothermics*, 22, 17-37.
- Tonani, F., 1973: Equilibria that control the hydrogen content of geothermal gases, Phillips Petroleum Co., Unpublished report. In: Carapezza, M., Nuccio, P. M., and Valenza, M. 1980, *Bull. Volcanol.* 44, 547-564.
- Truesdell, A.H., 1976: Summary of section III - geochemical techniques in exploration. *Proceedings of the 2nd U.N. Symposium on the Development and Use of Geothermal Resources, San Francisco*, 1, liii-lxxxix.
- Truesdell, A.H., and Fournier, R.O., 1977: Procedure for estimating the temperature of a hot water component in a mixed water using a plot of dissolved silica vs. enthalpy. *U.S. Geol. Survey J. Res.*, 5, 49-52.
- Wang J., Xiong L., and Pang Z., 1993: *Low-medium temperature geothermal system of convective type*. Science Press, Beijing, 240 pp.
- Zhao Ping, and Ármannsson, H., 1996: Gas geothermometry in selected Icelandic geothermal fields with comparative examples from Kenya. *Geothermics*, 25-3, 307-347.